Weierstraß-Institut
für Angewandte Analysis und Stochastik
Leibniz-Institut im Forschungsverbund Berlin e. V.

Preprint ISSN 2198-5855

The partial molar volume and area of solvated ions and some aspects of partial charge transfer

Manuel Landstorfer

submitted: November 22, 2016

Weierstrass Institute
Mohrenstr. 39
10117 Berlin
Germany
E-Mail: manuel.landstorfer@wias-berlin.de

No. 2337
Berlin 2016

2010 *Mathematics Subject Classification.* 78A57, 35Q35, 34B15.

2010 *Physics and Astronomy Classification Scheme.* 82.45.Gj, 68.43.-h, 68.35.Md.

Key words and phrases. Double layer, adsorption, solvation, surface mixture theory, partial charge transfer, electrode/electrolyte interface.

This work was supported by the Leibniz association.

Edited by
Weierstraß-Institut für Angewandte Analysis und Stochastik (WIAS)
Leibniz-Institut im Forschungsverbund Berlin e. V.
Mohrenstraße 39
10117 Berlin
Germany

Fax: +49 30 20372-303
E-Mail: preprint@wias-berlin.de
World Wide Web: http://www.wias-berlin.de/

Abstract

The double layer capacity is one of the central quantities in theoretical and experimental electrochemistry of metal/electrolyte interfaces. It turns out that the capacity is related to two central thermodynamic quantities, i.e. the partial molar volume of an ionic constituent and the partial molar area of the respective adsorbate. Since ions in solution (or on the surface) accumulated solvent molecules in their solvation shell, the partial molar volume and area are effected by this phenomena. In this work we discuss several aspects of the relationship between the molar volume and area of an ion, the solvation number and the charge number. In addition, we account for partial charge transfer on the metal surface which explains naturally the difference of the capacity maxima between F^- and ClO_4^- on silver. We provide simple yet validated analytical expressions for the partial molar volume and area of multi-valent ions and parameter values for aqueous solutions.

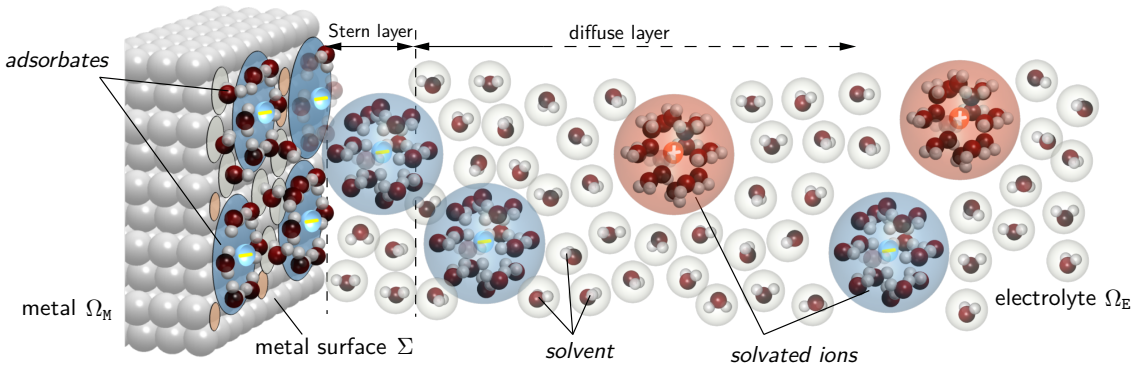

Figure 1: Sketch of the metal-electrolyte interface. The Stern-layer and the diffuse layer is self-consistently incorporated within the model. Solvent molecules are assumed to form a solvation shell around each ion, in the volume and on the surface.

1 Introduction

The partial molar volume v_α^R of a solvated ion A_α in solution and the partial molar area a_α^R of an ionic adsorbate $\underset{s}{\mathrm{A}}_\alpha$ are key parameters for the thermodynamic behavior of an electrochemical interface. Especially the electrochemical double layer electrolyte [1–3] is crucially influenced by these quantities.

A *fingerprint* of the double layer is the differential capacity C, which is in general a non-linear function of the measured cell voltage E (c.f. Fig. 2b). We derived recently a continuum thermodynamic model in [4] which is capable to predict qualitatively and quantitatively the capacity for various electrolytes and metal electrodes in a broad potential range (c.f. Fig. 2). The interfacial capacity C_E actually spreads in a boundary layer contribution C_E^BL, and a surface capacity $\underset{s}{C}_\mathrm{E}$, with $C_\mathrm{E} = C_\mathrm{E}^\mathrm{BL} + \underset{s}{C}_\mathrm{E}$, where $\underset{s}{C}_\mathrm{E}$ vanishes of no adsorption of ionic constituents occurs. We find that the maximum of the boundary layer capacity C_BL is non-linearly dependent on the value of the partial molar volume v_α^R (Fig. 3a) while the maximum of the surface capacity is determined by a_α^R (Fig. 3b).

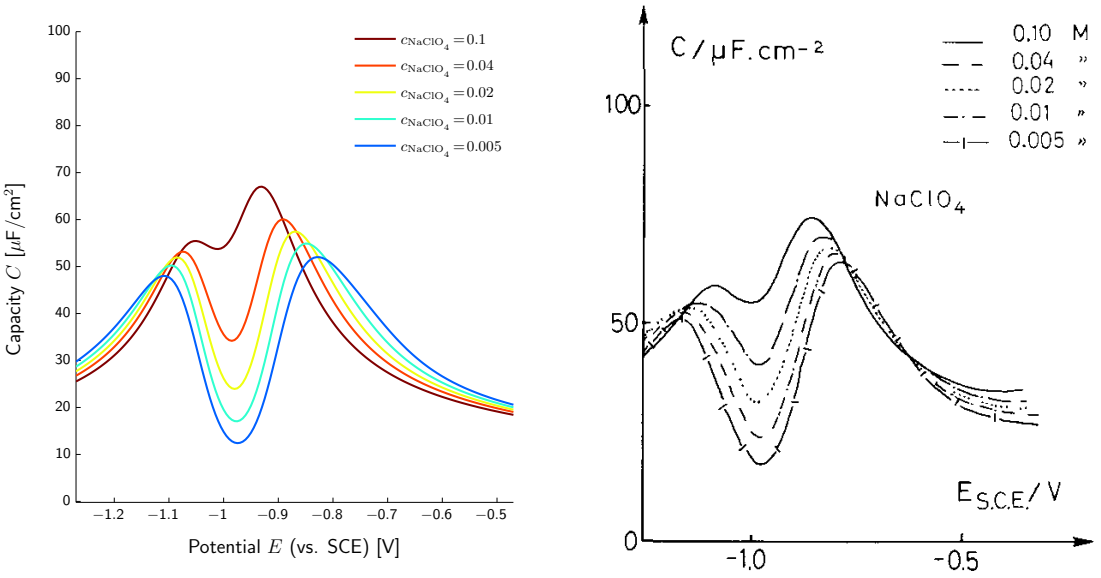

(a) Computed capacity based on the model given in [4].

(b) Measured capacity (Fig 2.b from [5], reprinted with permission from Elsevier)

Figure 2: Comparison of the computed capacity (a) and the measured capacity (b) of the Ag(110)| $\mathrm{NaClO_4}$ interface for concentrations of $(0.005 - 0.1)$M.

For non-adsorbing ionic solutions, e.g. $\mathrm{KPF_6}$ vs Ag [5], the capacity maximum is in the order of $50 - 60\,\mu\mathrm{F\,cm^{-2}}$, which requires that v_α^R of $\mathrm{K^+}$ and $\mathrm{PF_6^-}$ is about $30 - 50$ times larger than the partial molar volume v_0^R of the solvent and equal for the anion and the cation. For adsorbing ions on Ag , e.g. $\mathrm{F^-}$ or $\mathrm{ClO_4^-}$, we find find that the partial molar area is necessarily $5 - 30$ times larger that a_0^R of the solvent, however, with different values of $\mathrm{F^-}$ and $\mathrm{ClO_4^-}$.

Within this work we discuss these aspects in detail and provide some insight on the *required* values. First we briefly summarize the thermodynamic modeling procedure and the derivation of the charge/current relation. This leads to the structural decomposition of the double layer charge in an electrolytic boundary layer contribution, which is mainly determined by the partial molar volume, and an electrolytic surface charge contribution, which is dependent on the partial molar area.

We discuss then the partial molar volume and some structural effects due to packing densities. Further discussion on multi-valent ions is followed, leading to some relations between solvation number, partial molar volume, and ionic charge. For the adsorbed ionic species we introduce the concept of partial charge transfer within our modeling framework and discuss its impact on the partial molar area. Validation and interpretation is based on representative examples of capacity measurements and computations.

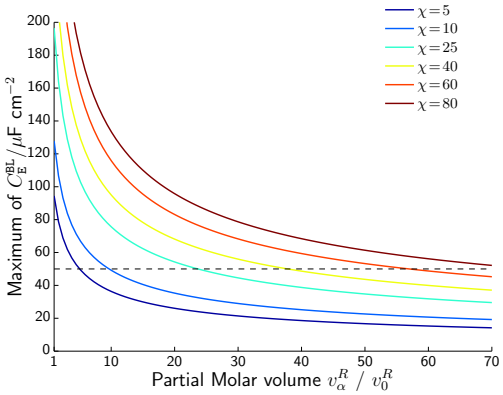

(a) Maximum of the boundary layer capacity C_{BL} as function of the molar volume v_α^R.

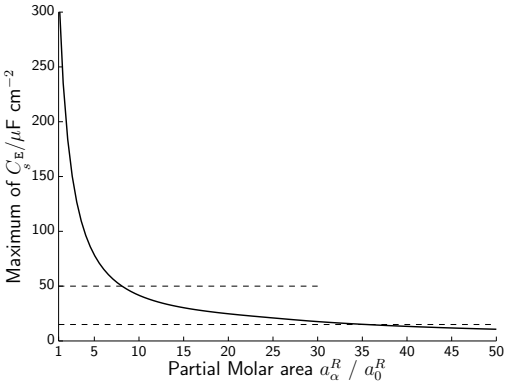

(b) Maximum of the surface capacity C_s as function of the ionic partial molar area a_α^R.

Figure 3: Maxima of the differential capacity contributions C_{BL} and C_s for a variation of the partial molar volume and area. The computations are based on the model of [4] for a 0.01M solution AC with an adsorbing anion.

2 Thermodynamic modeling

We consider a metal Ω_{M} in contact with an electrolytic solution Ω_{E}, sharing the common surface Σ. For this study we consider the approximation of a flat metal surface Σ positioned at $x = x_s$ and a homogenous distribution on the surface, i.e. a 1-D approximation.

Discontinuities at Σ of a quantity u are again denoted by $u\big|^- - u\big|^+ = [\![u]\!]$ and the bulk values in the metal and the electrolyte are $u_{\mathrm{M}} = u|_{x_{\mathrm{M}}}$ and $u_{\mathrm{E}} = u|_{x_{\mathrm{E}}}$, respectively. The framework of continuum thermo-electrodynamics for volumes and surfaces serves as basis for the modeling procedure [6–11]. It relies on general balance equations for the continuous field variables of mass, energy, and momentum as well as the electromagnetic field. The material specific modeling is carried out by constitutive equations of the free energy density $\rho\psi$ and ψ_s. Since the metal surface is explicitly taken into account as independent thermodynamic quantity, we require balance equations and thermodynamics of singular surfaces [7, 10–12].

2.1 Constituents and Balance equations

The electrolyte Ω_{E} is considered as a mixture of constituents $\mathrm{A}_\alpha\,, \alpha = 0, 1, \ldots, N_{\mathrm{E}}$ with molar mass m_α and charge $e_0 z_\alpha$, where A_0 denotes the solvent ($z_0 = 0$). For each constituent we have a (volume) density $n_\alpha(\mathbf{x}, t)\,/\,\mathrm{mol\,m^{-3}}$ which satisfies the global

balance equation (in the 1-D approximation)

$$\frac{d}{dt}\, n_\alpha^{\mathrm{BL}} = -j_\alpha\Big|_{x=x_{\underset{s}{}}} + j_\alpha\Big|_{x=x_{\mathrm{E}}} \quad \text{with} \quad n_\alpha^{\mathrm{BL}} := \int_{\underset{s}{x}}^{x_{\mathrm{E}}} n_\alpha \, dx, \quad \alpha = 0, 1, \ldots, N_{\mathrm{E}}\,, \tag{1}$$

where j_α is the molar flux of A_α in positive x-direction. The total mass density of the electrolyte is $\rho_{\mathrm{E}} = \sum_{\alpha=0}^{N_{\mathrm{E}}} m_\alpha n_\alpha$, the charge density $q_{\mathrm{E}} = e_0 \sum_{\alpha=1}^{N_{\mathrm{E}}} z_\alpha n_\alpha$, and the electrolyitc boundary layer charge

$$q_{\mathrm{E}}^{\mathrm{BL}} = \int_{\underset{s}{x}}^{x_{\mathrm{E}}} q_{\mathrm{E}} \, dx \ . \tag{2}$$

We consider the metal Ω_{M} as mixture of metal ions A_M (with charge number z_M) and valance electrons A_e in terms of species (volume) densities $n_\alpha(\mathbf{x}, t)\,/\,\mathrm{mol\,m^{-3}}$ and the corresponding global balance equations are similar to (1).

On the metal surface Σ we consider adsorption of all constituents from the metal **and** the electrolyte phase in terms of species densities $\underset{s}{n}_\alpha(\underset{s}{\mathbf{x}}, t)\,/\,\mathrm{mol\,m^{-2}}$, satisfying the global surface balance equations

$$\frac{d}{dt}\underset{s}{n}_\alpha = j_\alpha\Big|_{x=x_{\underset{s}{}}} + \underset{s}{r}_\alpha \qquad \alpha = 0, 1, \ldots, N_{\mathrm{E}}\,, \tag{3}$$

with surface reaction rate $\underset{s}{r}_\alpha$. Since these adsorbates may react further on the surface, we have in addition $\underset{s}{\mathrm{A}}_\alpha = N_{\mathrm{E}+1}, \ldots, N_{\mathrm{S}}$ exclusive surface species which satisfy the balance equations

$$\frac{d}{dt}\,\underset{s}{n}_\alpha = \underset{s}{r}_\alpha \qquad \alpha = N_{\mathrm{E}} + 1, \ldots, N_S \ . \tag{4}$$

The surface charge density $\underset{s}{q}$ is thus

$$\underset{s}{q} = \underset{s}{q}_{\mathrm{M}} + \underset{s}{q}_{\mathrm{E}} \quad \text{with} \quad \underset{s}{q}_{\mathrm{M}} = e_0(\underset{s}{z}_M \underset{s}{n}_M - \underset{s}{n}_e) \quad \text{and} \quad \underset{s}{q}_{\mathrm{E}} = e_0 \sum_{\alpha=1}^{N_{\mathrm{S}}} \underset{s}{z}_\alpha \underset{s}{n}_\alpha \ , \tag{5}$$

where $\underset{s}{z}_\alpha$ denotes the surface charge number of the respective species.

2.2 Surface Reactions

We consider in general the following reactions:

- **Adsorption**
  corresponds to the diffusion or jump process from a point $x \to x_S$ onto the surface Σ.

$$\mathrm{A}_\alpha \rightleftharpoons \underset{s}{\mathrm{A}}_{\alpha,-1} \ , \qquad \alpha = 0, \ldots, N_{\mathrm{E}} \tag{6}$$

  The charge number z_α, mass m_α and solvation number κ_α remain equal. Note that we abbreviate the adsorbed solvent also by $\underset{s}{\mathrm{A}}_0$.

- **Partial charge transfer and de-solvation**
  describes the restructuring and release of solvent molecules of the ions after the adsorption process occurred. This process could occur simultaneously with the transfer of a partial charge from some valence electrons. We denote by $(\underset{s}{A}_{1,0}, \dots, \underset{s}{A}_{N_{\mathrm{E}},0})$ the reaction products of this process and write the general reactions as

$$\underset{s}{\mathrm{A}}_{\alpha,-1} + \mathrm{sgn}(z_\alpha)\lambda_{\alpha,0}\, \underset{s}{\mathrm{e}}^- \rightleftharpoons \underset{s}{A}_{\alpha,0} + (\kappa_\alpha - \kappa_{\alpha,0})\, \underset{s}{A}_0\ ,\ \alpha = 1, \dots, N_{\mathrm{E}}, \tag{7}$$

  where $\lambda_{\alpha,0}$ denotes the partial charge transfer coefficient and $\underset{s}{R}_{\alpha,\beta}$ the reaction rate. Correspondingly, the charge of the constituent $\underset{s}{A}_{\alpha,0}$ is $z_{\alpha,0} = z_\alpha - \mathrm{sgn}(z_\alpha)\lambda_{\alpha,0}$ and the solvation number $\kappa_{\alpha,0}$. Hence, the species $\underset{s}{A}_{\alpha,0}$ are partially solvated, adsorbed ions. Note that $\lambda_{\alpha,0}$ could also be zero. The last term in (7) accounts for the shrinking of the solvation shell and thus the release of solvent molecules $\underset{s}{A}_0$ on the surface.

- **Subsequent partial electron transfer**
  models the transfer of electrons from the metal onto the reaction products of (7). The first (partial) electron is transferred from (or to) a partially solvated ion $\underset{s}{A}_{\alpha,0}$, producing a species $\underset{s}{A}_{\alpha,1}$ with charge number $z_{\alpha,1} = z_{\alpha,0} - \mathrm{sgn}(z_\alpha)\, \lambda_{\alpha,1}$ and solvation number $\kappa_{\alpha,1}$. This species $\underset{s}{A}_{\alpha,1}$ could further react with a partial electron to produce a constituent $\underset{s}{A}_{\alpha,2}$, and so forth. The general scheme is thus

$$\underset{s}{A}_{\alpha,\beta-1} + \mathrm{sgn}(z_\alpha)\lambda_{\alpha,\beta}\, \underset{s}{\mathrm{e}}^- \rightleftharpoons \underset{s}{A}_{\alpha,\beta} + (\kappa_{\alpha,\beta-1} - \kappa_{\alpha,\beta})\underset{s}{A}_0 \tag{8}$$

  for $\beta = 1, \dots, |z_\alpha|,\ \alpha = 1, \dots, N_{\mathrm{E}}$ with reaction rate $\underset{s}{R}_{\alpha,\beta}$. The species $\underset{s}{A}_{\alpha,\beta}$ has then a charge number $\underset{s}{z}_{\alpha,\beta} = z_\alpha - \mathrm{sgn}(z_\alpha) \sum_{\gamma=0}^{\beta} \lambda_{\alpha,\gamma}$ solvation number $\kappa_{\alpha,\beta}$.

In some sense, the de-solvation and the electron transfer reaction *smear* to one type of surface reaction. Further,

$$\lambda_\alpha^\beta := \sum_{\gamma=0}^{\beta} \lambda_{\alpha,\gamma} \qquad \beta = 1, \dots, |z_\alpha|,\ \alpha = 1, \dots, N_{\mathrm{E}} \tag{9}$$

corresponds to the *effective* charge transfer number due to the β electron transfer reactions. If only integers of electrons are transferred we have $\lambda_\alpha^\beta = \beta$.

2.3 Current-charge relation

The current density I which flows out of the the metal, i.e. through the boundary $\partial\Omega_{\mathrm{M}}$, is denoted by

$$I = e_0(z_M j_M - j_e)\Big|_{x=x_{\mathrm{M}}} \tag{10}$$

Insertion of the global balance equations for the electrons and the metal ions of the volume (1) and the surface (3), as well as the global electroneutrality condition

$$q_{\mathtt{M}}^{\mathtt{BL}} + \underset{s}{q_{\mathtt{M}}} + \underset{s}{q_{\mathtt{E}}} + q_{\mathtt{E}}^{\mathtt{BL}} = 0 \tag{11}$$

gives

$$I = -\frac{d}{dt}\left(q_{\mathtt{E}}^{\mathtt{BL}} + \underset{s}{q_{\mathtt{E}}}\right) + e_0\, \underset{s}{r_e}\ , \tag{12}$$

where $\underset{s}{r_e}$ denotes the production/annihilation of surface electrons. Since these electrons are involved in the (partial) electron transfer reactions (7) and (8), we habe

$$r_e = -\sum_{\alpha=1}^{N_{\mathtt{E}}} \sum_{\beta=0}^{|z_\alpha|} \mathsf{sgn}(z_\alpha) \lambda_{\alpha,\beta} \underset{s}{R_{\alpha,\beta}}\ . \tag{13}$$

Each adsorbate $\underset{s}{\mathrm{A}_{\alpha,\beta}}$ is involved in two surface reactions, whereby the surface production density $r_{\alpha,\beta}$ is represented by

$$r_{\alpha,\beta} = (R_{\alpha,\beta} - R_{\alpha,\beta+1}) \tag{14}$$

with $R_{\alpha,|z_\alpha|+1} = 0$. We can thus write

$$R_{\alpha,\beta} = r_{\alpha,|z_\alpha|} + r_{\alpha,|z_\alpha|-1} + \cdots + r_{\alpha,|z_\alpha|-\beta}\ . \tag{15}$$

which leads after some rearrangement to

$$r_e = -\sum_{\alpha=1}^{N_{\mathtt{E}}} \sum_{\beta=0}^{|z_\alpha|} \mathsf{sgn}(z_\alpha) \lambda_\alpha^\beta\, r_{\alpha,\beta} = -\sum_{\alpha=1}^{N_{\mathtt{E}}} \sum_{\beta=0}^{|z_\alpha|} \mathsf{sgn}(z_\alpha) \lambda_\alpha^\beta \frac{\partial \underset{s}{n_{\alpha,\beta}}}{\partial t}\ . \tag{16}$$

We obtain thus finally

$$I = \frac{dQ}{dt} \quad \text{with} \quad Q = -q_{\mathtt{E}}^{\mathtt{BL}} - \underset{s}{q_{\mathtt{E}}^{\mathsf{Eff}}} \quad \text{and} \quad \underset{s}{q_{\mathtt{E}}^{\mathsf{Eff}}} = e_0 \sum_{\alpha=1}^{N_{\mathtt{E}}} z_\alpha \sum_{\beta=-1}^{|z_\alpha|} \underset{s}{n_{\alpha,\beta}}\ . \tag{17}$$

Here, $q_{\mathtt{E}}^{\mathtt{BL}}$ corresponds to the boundary layer charge of the electrolytic solution while $\underset{s}{q_{\mathtt{E}}^{\mathsf{Eff}}}$ corresponds to the *effective* surface charge of electrolytic adsorbates on the metal. The term *effective* is used to emphasize that the pseudo-charge

$$\underset{s}{q_{\mathtt{E}}^{\mathsf{PS}}} := \sum_{\alpha=1}^{N_{\mathtt{E}}} \sum_{\beta=0}^{|z_\alpha|} \mathsf{sgn}(z_\alpha) \lambda_\alpha^\beta \underset{s}{n_{\alpha,\beta}} \tag{18}$$

of the partial charge transfer reactions is also incorporated in $\underset{s}{q_{\mathtt{E}}^{\mathsf{Eff}}}$, i.e. $\underset{s}{q_{\mathtt{E}}^{\mathsf{Eff}}} = \underset{s}{q_{\mathtt{E}}^{\mathsf{PS}}} + \underset{s}{q_{\mathtt{E}}}$.

Note that the partial charge transfer coefficients $\lambda_{\alpha,\beta}$ do not arise anymore in (17). The pre-factor of $\underset{s}{n_{\alpha,\beta}}$ in (17) is z_α and not $\underset{s}{z_{\alpha,\beta}} \propto \lambda_\alpha^\beta$. This is a crucial aspect of the partial charge transfer since it shows that one is not able to directly measure λ_α^β, which is in accordance to the finding of Schmickler and others [13, 14].

However, λ_α^β certainly has an impact on some thermodynamic parameters of the adsorbates $\underset{s}{\mathrm{A}_{\alpha,\beta}}$, which are incorporated in the respective chemical potentials.

2.4 Chemical potentials

The chemical potentials of some constituent A_α are derived based on some explicit free energy functions. Within the theory of coupled volume and surface thermodynamics, independent free energy densities of the volume, i.e. $\rho\psi$, and the surface, $\underset{s}{\psi}$, arise. The derivation of these free energy functions is not scope of this work, and the detailed derivation is given in [4]. The chemical potentials of some constituent A_α in the volume and on the surface are

$$\mu_\alpha = \frac{\partial \rho\psi}{\partial n_\alpha} \quad \text{and} \quad \underset{s}{\mu_\alpha} = \frac{\partial \underset{s}{\psi}}{\partial \underset{s}{n_\alpha}} \,. \tag{19}$$

For the electrolyte phase we rely on the free energy density $\rho\psi^{\mathtt{E}}$ given in [4] which covers the entropy of mixing, solvation effects as well as the incompressibility of the liquid mixture. The chemical potentials of the respective constituents are

$$\mu_\alpha = \frac{\partial \rho\psi^{\mathtt{E}}}{\partial n_\alpha} = g_\alpha^R + k_{\mathtt{B}} T \, \ln y_\alpha + v_\alpha^R (p - p^{\mathtt{E}}) \qquad \alpha = 0, 1, \ldots, N_{\mathtt{E}}, \tag{20}$$

where g_α^R denotes the reference partial molar Gibbs energy, $y_\alpha = \frac{n_\alpha}{n}$ the mole fraction, $n = \sum_{\alpha=0}^{N} n_\alpha$ the number density of mixing particles[1], v_α^R the partial molar volume, and p is the pressure. Note that the incompressibility of the liquid mixture implies the constraint

$$n = \frac{1}{\sum_{\alpha=0}^{N} v_\alpha^R y_\alpha} \,. \tag{21}$$

The metal is modeled as Thomas–Fermi electron gas with free energy density $\rho\psi^{\mathtt{M}}$ of [4] with representations

$$\mu_M = \frac{\partial \rho\psi^{\mathtt{M}}}{\partial n_M} = g_M^R + v_M^R (p_M - p_M^R) \quad \text{and} \quad \mu_e = \frac{\partial \rho\psi^{\mathtt{E}}}{\partial n_e} = \frac{h^2}{2m_e} \left(\frac{3}{8\pi}\right)^{\frac{2}{3}} n_e^{\frac{2}{3}} \,, \tag{22}$$

where v_M^R denotes the partial molar volume of the metal ions, p_M the metal ion partial pressure, g_M^R the reference Gibbs energy and p_M^R the bulk pressure. The incompressibility implies $v_M^R = 1/n_M$.

On the surface we consider a surface free energy density $\underset{s}{\psi}$ which covers surface solvation effects, surface incompressibility, entropy of mixing, and reference contributions [4]. With the explicit representation of $\underset{s}{\psi}$ given in [4] we obtain the surface chemical potentials

$$\underset{s}{\mu_\alpha} = \frac{\partial \underset{s}{\psi}}{\partial \underset{s}{n_\alpha}} = \begin{cases} \underset{s}{\psi_\alpha^R} + k_B T \ln \underset{s}{y_\alpha} - \overline{\omega}_\alpha k_B T \ln \underset{s}{y_V} & \text{for } \alpha = 0, 1, \ldots, N_S \\ \underset{s}{\psi_M^R} + \overline{\omega}_M k_B T \ln \underset{s}{y_V} - a_M^R \underset{s}{\gamma^{\mathtt{E}}} & \text{for } \alpha = \mathrm{M}^+ \\ \underset{s}{\psi_e^R} = \text{const.} & \text{for } \alpha = \mathrm{e}^- . \end{cases} \tag{23}$$

[1] Note that due to the solvation effect not all solvent molecules participate in the entropy of mixing. Since each ion binds κ_α solvent molecules, n_0 actually denotes the *free* solvent molecules, while $n_0^t = n_0 + \sum_{\alpha=1}^{N} \kappa_\alpha n_\alpha$ denotes the *total* number density of solvent in the mixture.

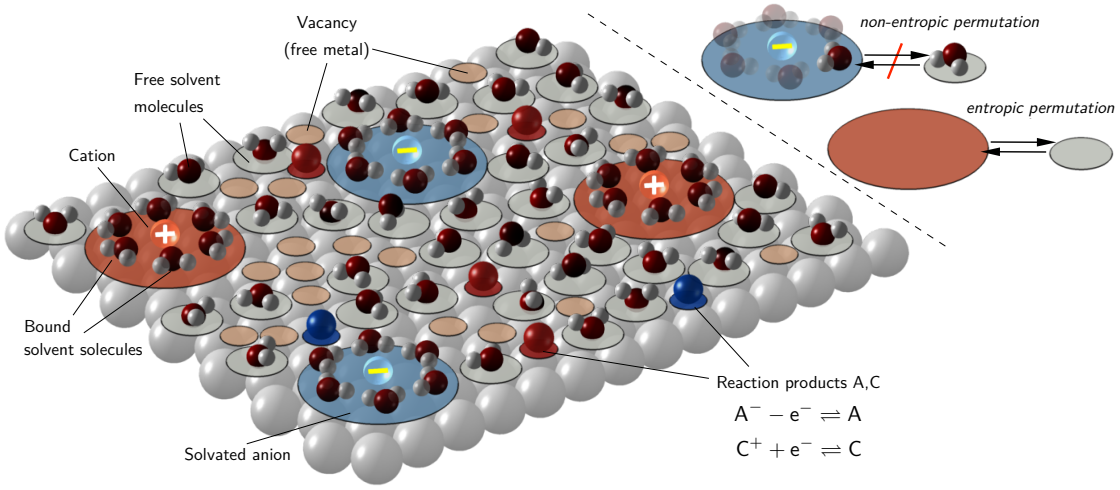

Figure 4: Sketch of the mixing particles on the metal surface. Note that the number of mixing particles is actually smaller than the actual number of molecules on the surface, since a solvated adsorbate counts entropically as one particle.

The respective quantities are

- the number of surface vacancies

$$\underset{s}{n}_V = \overline{\omega}_M \underset{s}{n}_M - \sum_{\alpha=0}^{N_S} \overline{\omega}_\alpha \underset{s}{n}_\alpha \ , \tag{24}$$

  where $\overline{\omega}_\alpha$ denotes the number of adsorption sites of $\underset{s}{\mathrm{A}}_\alpha$,

- the number of mixing particles

$$\underset{s}{n} = \underset{s}{n}_V + \sum_{\alpha=0}^{N_S} \underset{s}{n}_\alpha \ , \tag{25}$$

- the surface fractions

$$\underset{s}{y}_\alpha = \frac{\underset{s}{n}_\alpha}{\underset{s}{n}} \qquad , \alpha = 0, 1, \ldots, N_S, V \ , \tag{26}$$

- the adsorbate surface tension γ^{E},
- the partial molar area of the metal surface a_M^R,
- and the constant electron surface chemical potential $\underset{s}{\psi}_e^R$.

The surface incompressibility implies quite similar to (21) the constraint

$$\underset{s}{n}_M = \frac{1}{a_M^R} \quad \Leftrightarrow \quad a_V^R \underset{s}{n}_V + \sum_{\alpha=0}^{N_S} a_\alpha^R \underset{s}{n}_\alpha = 1 \tag{27}$$

with the partial molar areas

$$a_V^R = \frac{1}{\overline{\omega}_M} a_M^{\mathtt{R}} \quad \text{and} \quad a_\alpha^R = \frac{\overline{\omega}_\alpha}{\overline{\omega}_M} a_M^{\mathtt{R}} = \overline{\omega}_\alpha a_V^R \ . \tag{28}$$

Note that we can thus either consider the number of adsorption sites $\overline{\omega}_\alpha$ or the molar areas a_α^R as model parameter. Our discussion in section 4 is based on a_α^R which turns out to be more convenient.

2.5 Equilibrium conditions

In the thermodynamic equilibrium, the following conditions hold [4]

- Diffusional equilibrium

$$\nabla \mu_\alpha + e_0 z_\alpha \nabla \varphi = 0 \qquad \alpha = 0, 1, \ldots, N_{\mathtt{E}} \tag{29}$$

- Adsorption equilibrium at Σ

$$\mu_\alpha|_S^+ = \underset{s}{\mu}_{\alpha,-1} \qquad \alpha = 1, \ldots, N_{\mathtt{E}} \quad \text{and} \quad \mu_\alpha|_S^- = \underset{s}{\mu}_\alpha \qquad \alpha = e, M. \tag{30}$$

- Electrical equilibrium

$$\varepsilon_0 \mathsf{div}\,(1+\chi)\mathbf{E} = q^{\mathsf{F}} \qquad \text{and} \qquad \varepsilon_0 [\![(1+\chi)\mathbf{E}]\!] = \underset{s}{q} \tag{31}$$

  with $\mathbf{E} = -\nabla\varphi$.

- Mechanical equilibrium in $\Omega^\pm$

$$\nabla p = -q^{\mathsf{F}} \nabla \varphi \qquad \text{and} \qquad [\![p]\!] = \underset{s}{q} \cdot \frac{1}{2}(\nabla\varphi|_\Sigma^+ - \nabla\varphi|_\Sigma^-) \tag{32}$$

- Surface reaction equilibrium on Σ

$$\underset{s}{\mu}_{\alpha,\beta-1} + \mathsf{sgn}(z_\alpha)\lambda_{\alpha,\beta} \underset{s}{\mu}_e = \underset{s}{\mu}_{\alpha,\beta} + (\kappa_{\alpha,\beta-1} - \kappa_\alpha, \beta)\underset{s}{\mu}_0 \ , \tag{33}$$

  for $\beta = 0, 1, \ldots, |z_\alpha| \,,\ \alpha = 1, \ldots, N_{\mathtt{E}}$.

Throughout this work we consider only equilibrium situations. Note that a combination of diffusional and adsorption equilibrium leads to

$$\mu_\alpha^{\mathtt{E}} + e_0 z_\alpha U^{\mathtt{E}} = \underset{s}{\mu}_{\alpha,-1} \qquad \alpha = 0, 1, \ldots, N_{\mathtt{E}}. \tag{34}$$

with $U_{\mathtt{E}} = \varphi|_\Sigma^+ - \varphi^{\mathtt{E}}$. We abbreviate the electrochemical potential as $\widetilde{\mu}_\alpha := \mu_\alpha + e_0 z_\alpha \varphi$.

2.6 Boundary layer charge representation

In [4] we derived in detail the representation of the boundary layer charge $q_{\mathrm{E}}^{\mathrm{BL}}$ in terms of the electrolytic boundary layer drop U^{E}. Briefly summarized we obtain from the electrical equilibrium (31) and the mechanical equilibrium (32) the representation

$$q_{\mathrm{E}}^{\mathrm{BL}} = \mathrm{sgn}(U^{\mathrm{E}})\sqrt{2\varepsilon_0(1+\chi)(p\big|_{\Sigma}^{+} - p^{\mathrm{E}})} \tag{35}$$

where $p\big|_{\Sigma}^{+}$ denotes the material pressure at the interface $x = 0^{+}$. From the diffusional equilibrium (29) we obtain representations

$$y_\alpha = y_\alpha^{\mathrm{E}} \cdot \mathrm{e}^{-z_\alpha \frac{e_0}{k_{\mathrm{B}}T}(\varphi(x)-\varphi^{\mathrm{E}}) - \frac{v_\alpha^R}{k_{\mathrm{B}}T}(p(x)-p^{\mathrm{E}})}\,. \tag{36}$$

which form together with the constraint

$$\sum_{\alpha=0}^{N_{\mathrm{E}}} y_\alpha = 1 \tag{37}$$

an implicit equation system

$$g(p\big|_{\Sigma}^{+}, U^{\mathrm{E}}) =: \sum_{\alpha=0}^{N_{\mathrm{E}}} y_\alpha\Big|_{\Sigma}^{+} - 1 = 0 \tag{38}$$

This allows us to deduce an implicit solution

$$p\big|_{\Sigma}^{+} = \hat{p}(U^{\mathrm{E}}) \tag{39}$$

and thus a representation

$$q_{\mathrm{E}}^{\mathrm{BL}} = \mathrm{sgn}(U^{\mathrm{E}})\sqrt{2\varepsilon_0(1+\chi)(\hat{p}(U^{\mathrm{E}}) - p^{\mathrm{E}})} = \hat{q}_{\mathrm{E}}^{\mathrm{BL}}(U^{\mathrm{E}}). \tag{40}$$

2.7 Effective surface charge representation

The equilibrium condition (33) of the reactions (7) and (8) (together with the adsorption and diffusional equilibrium in the electrolyte) can be summarized as

$$\mu_\alpha^{\mathrm{E}} + e_0 z_\alpha U^{\mathrm{E}} + \mathrm{sgn}(z_\alpha)\lambda_\alpha^\beta \underset{s}{\mu}_e = \underset{s}{\mu}_{\alpha,\beta} + (\kappa_{\alpha,\beta} - \kappa_\alpha)\mu_0^{\mathrm{E}}\,, \tag{41}$$

for $\beta = -1, 0, 1, \ldots, |z_\alpha|$, $\alpha = 1, \ldots, N_{\mathrm{E}}$. With the representation (23) of the surface chemical potential $\underset{s}{\mu}_{\alpha,\beta}$ we obtain the representations ($\beta = -1, 0, 1, \ldots, |z_\alpha|$)

$$\underset{s}{y}_{\alpha,\beta} = y_\alpha^{\mathrm{E}}(y_0^{\mathrm{E}})^{(\kappa_{\alpha,\beta}-\kappa_\alpha)}\mathrm{e}^{-\frac{\Delta g_{\alpha,\beta}^A}{k_B T} - \frac{z_\alpha e_0}{k_B T}U^{\mathrm{E}} + \frac{a_{\alpha,\beta}^R}{k_B T}\gamma^{\mathrm{E}}} \qquad \alpha = 1, \ldots, N_{\mathrm{E}}, \tag{42}$$

with *adsorption energy*

$$\Delta g^A_{\alpha,\beta} = \Delta \widetilde{g}^R_{\alpha,\beta} + \kappa_{\alpha,\beta} \Delta \widetilde{g}^R_0 \tag{43}$$

$$\text{and} \quad \Delta \widetilde{g}_{\alpha,\beta} = \underset{s}{\widetilde{\psi}^R_{\alpha,\beta}} - \underset{s}{\widetilde{g}^R_\alpha} - \mathrm{sgn}(z_\alpha) \lambda^\beta_\alpha \cdot \underset{s}{\mu_e} \quad , \quad \Delta \widetilde{g}_0 = (\psi^R_0 - g^R_0) \ . \tag{44}$$

Note that the functional representation (42) of $\underset{s}{y_{\alpha,\beta}}$ is exactly the same as the one obtained for integer charge transfer reactions [4]

$$\underset{s}{A_{\alpha,\beta-1}} + \mathrm{sgn}(z_\alpha) \underset{s}{A_e} \rightleftharpoons \underset{s}{A_{\alpha,\beta}} + (\kappa_{\alpha,\beta-1} - \kappa_{\alpha,\beta}) \underset{s}{A_0} \ . \tag{45}$$

The pre-factor of $U^{\mathtt{E}}$ in the representation (42) is z_α, and **not** $\underset{s}{z_{\alpha,\beta}} = z_\alpha - \mathrm{sgn}(z_\alpha)\lambda^\beta_\alpha$. Hence, the only difference between adsorbates with partial and integer charge on the surface can be *parametrically* with respect to the

- partial molar area $a_{\alpha,\beta}$ (or the the surface solvation number $\kappa_{\alpha,\beta}$),
- and the adsorption energy $\Delta \widetilde{g}^A_{\alpha,\beta}$.

Quite similar to the volume we have on the surface the implicit equation system

$$\underset{s}{g}(\gamma^{\mathtt{E}}, U^{\mathtt{E}}) := \underset{s}{y_{\mathtt{V}}} + \sum_{\alpha=0}^{N_{\mathtt{E}}} \sum_{\beta=-1}^{|z_\alpha|} \underset{s}{y_{\alpha,\beta}} - 1 = 0 \tag{46}$$

with the representations (42) for $\underset{s}{y_{\alpha,\beta}}$ and

$$\underset{s}{y_V} = \mathrm{e}^{-\frac{a^R_M}{k_B T} \underset{s}{\gamma^{\mathtt{E}}}} \quad , \tag{47}$$

which determines $\gamma^{\mathtt{E}} = \hat{\gamma}^{\mathtt{E}}(U^{\mathtt{E}})$. Together with (27) and (42) we obtain thus for the effective surface charge a representation

$$\underset{s}{q^{\mathsf{Eff}}_{\mathtt{E}}} = \frac{e_0 \sum_{\alpha=1}^{N_{\mathtt{E}}} \sum_{\beta=-1}^{|z_\alpha|} z_\alpha \, y_{\alpha,\beta}}{a^R_M y_V + \sum_{\alpha=0}^{N_{\mathtt{E}}} \sum_{\beta=-1}^{|z_\alpha|} a^R_{\alpha,\beta} \, y_{\alpha,\beta}} = \underset{s}{\hat{q}^{\mathtt{E}}}(U^{\mathtt{E}}) \ . \tag{48}$$

2.8 Measured cell potential

We consider the metal-electrolyte interface in contact to some reference electrode $\mathtt{R}$, where the two metals are connected in an outer circuit to a potentiostat/voltmeter which measures the voltage E. Due to the continuity of electrochemical potential $\widetilde{\mu}_e$ of the electrons we have [4]

$$E = -(\widetilde{\mu}^{\mathtt{R}}_e - \widetilde{\mu}^{\mathtt{M}}_e) = U^{\mathtt{E}} + U^{\mathtt{R}} \quad \text{with} \quad U^{\mathtt{R}} = -\frac{1}{e_0}(\underset{s}{\mu^{\mathtt{M}}_e} - \underset{s}{\mu^{\mathtt{R}}_e}) - U^{\mathtt{R,E}} \tag{49}$$

where $U^{\mathtt{R,E}} = \underset{s}{\varphi^{\mathtt{R}}} - \varphi^{\mathtt{E}}$ denotes the potential difference between bulk electrolyte and surface potential of the reference electrode. The reference electrode is considered as *ideally non-polarizable (reference) electrode* [15], which states $U^{\mathtt{R,E}} = \text{const}$. We have thus an explicit relation between the measurable cell potential E and the electrolyte potential drop $U^{\mathtt{E}}$. Note further that we can consider $U^{\mathtt{R}}$ as parameter instead of $\underset{s}{\mu^{\mathtt{M}}_e}$.

2.9 Capacity

The capacity of the electrochemical interface is obtained from a quasi-stationary thermodynamic process, i.e. $E = E(t)$, such that the thermodynamic equilibrium conditions (29) - (32) hold for each time-step. The equilibrium representations of the boundary layer and surface charge, i.e.

$$Q = -\hat{q}_{\mathrm{E}}^{\mathrm{BL}}(E - U^{\mathrm{R}}) - \underset{s}{q}_{\mathrm{E}}^{\mathsf{Eff}}(E - U^{\mathrm{R}}) = \hat{Q}(E - U^{\mathrm{R}}) \ , \tag{50}$$

thus lead to

$$I = \frac{dQ}{dt} = C \cdot \frac{dE}{dt} \quad \text{with} \quad C = C_{\mathrm{E}}^{\mathrm{BL}} + \underset{s}{C}_{\mathrm{E}}^{\mathsf{Eff}} \ , \tag{51}$$

$$C_{\mathrm{BL}}^{\mathrm{E}} = -\frac{dq_{\mathrm{E}}^{\mathrm{BL}}}{dE} \quad \text{and} \quad \underset{s}{C}_{\mathrm{E}}^{\mathsf{Eff}} = -\frac{d\underset{s}{q}_{\mathrm{E}}^{\mathsf{Eff}}}{dE} \ . \tag{52}$$

We call $C \,/\, \mathrm{F\ m^{-2}}$ differential capacity of the interface and accordingly $C_{\mathrm{E}}^{\mathrm{BL}}$ boundary layer capacity and $\underset{s}{C}_{\mathrm{E}}^{\mathsf{Eff}}$ effective surface capacity. The functional representation of $C_{\mathrm{E}}^{\mathrm{BL}}$ is given in A.1 and of $\underset{s}{C}_{\mathrm{E}}^{\mathsf{Eff}}$ in A.2.

We performed already a validation study of this model in [4], which showed a broad qualitative and quantitative agreement to experimental data. Here, however, we want to discuss certain aspects of the necessary model parameters.

3 Partial molar volume

The solvation effect [16–22], i.e. the *binding* of solvent molecules to the central ion due to microscopic electrostatic interactions, is a key feature for the thermodynamic behavior of an electrolytic mixture. Due to this effect, the partial molar volume v_α^R of an ionic constituent A_α incorporates the *volume* of κ_α solvent molecules A_0. The most simple relationship between these two quantities is [4, 23]

$$v_\alpha^R = (1 + \kappa_\alpha)\, v_0^R \ , \tag{53}$$

which assumes a constant density upon solvation. Based on the relation (53) one could then estimate the solvation number κ_α for a given value of v_α^R. We find that the solvation number has to be in the order of[2] $\kappa_\alpha \approx 25 - 60$ (for mono-valent ions) in order to agree with capacity measurments of some non-adsorbing salt (c.f. Fig. 5 in comparison to Fig. 7). Such large values might seem disappointing, even though they account for the first and second solvation shell. But predictions on solvation numbers are still in discussion [24] and various values can be found in the literature [18].

Requisitioning the relation (53) in terms of a microscopic structure model shows that the model perception $v_\alpha^R = (1+\kappa_\alpha)\, v_0^R$ actually neglects packing effects in the solvation

[2] The capacity maximum depends also on the chosen value for the electrolytic susceptibility χ^{E} .

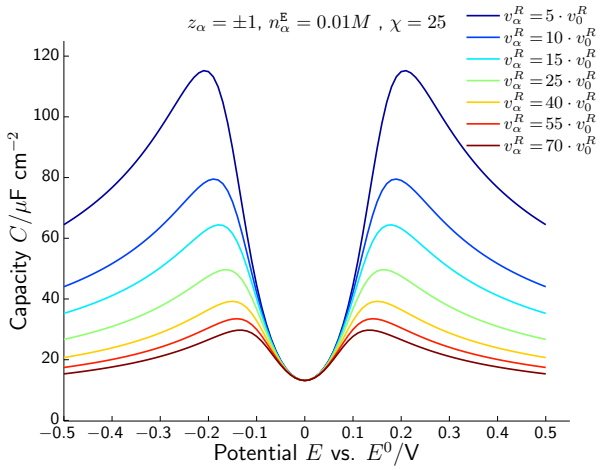

Figure 5: Computed capacity for a non-adsorbing salt AC with bulk concentration $0.01\,/\,\mathrm{mol\,L^{-1}}$.

shell [25, 26]. Since the packing fraction p ranges from 0.42 for a octahedral geometry down to 0.33 for a hexagonal bi-pyramide, it dramatically reduces the *number* of solvent molecules in the solvation shell for a given volume v_α^R.

Consider the case of an octahedral molecular geometry **S1** for a solvated ion (see Fig. 6). The solvent molecules form a structural solvation shell (i.e. the first solvation shell) around the central ion. The radius of the solvent *sphere* in the solvation shell is $\widetilde{r}_0$ and in the range of $1 - 2\text{Å}$. An approximate value of $\widetilde{r}_0$ can be determined from the partial molar volume of the solvent, i.e.

$$\widetilde{r}_0 \approx r_0 = \sqrt[3]{\frac{3}{4\pi} v_0^R} \approx 1.92\ /\,\text{Å} \quad \text{with} \quad v_0^R = \frac{1}{55.5}\,/\,\frac{\mathsf{L}}{\mathsf{mol}}\ . \tag{54}$$

Presumably the radius $\widetilde{r}_0$ within the dipolar bond of the solvation shell is smaller than the molar radius r_0. However, for the introduction of the packing fraction the approximation $\widetilde{r}_0 \approx r_0$ is quite sufficient.

From the structure model **S1** we can determine the radius of the circumscribed sphere as $r_{\mathsf{cs}} = (1 + \sqrt{2})\, r_0$, leading to the volume $V_{\mathsf{cs}} = \frac{4}{3}\pi(1 + \sqrt{2})^3 r_0^3$. The packing factor p is then the number of molecules within the circumscribed sphere, times the volume of the solvent sphere V_0, divided by volume of the circumscribed sphere. Note that we assume here that the radius of the central ion is smaller than the radius of the solvent spheres. Since the number of solvent molecules is actually the solvation number κ_α, we have for the octahedral structure model a packing factor of

$$p = \frac{(1 + \kappa_\alpha) V_0}{V_{\mathsf{cs}}} = 0.4975\ . \tag{55}$$

Since the fraction $\frac{V_0}{V_{\mathsf{cs}}}$ is equal to the fraction of the partial molar volumes, $\frac{v_0^R}{v_\alpha^R}$ (for

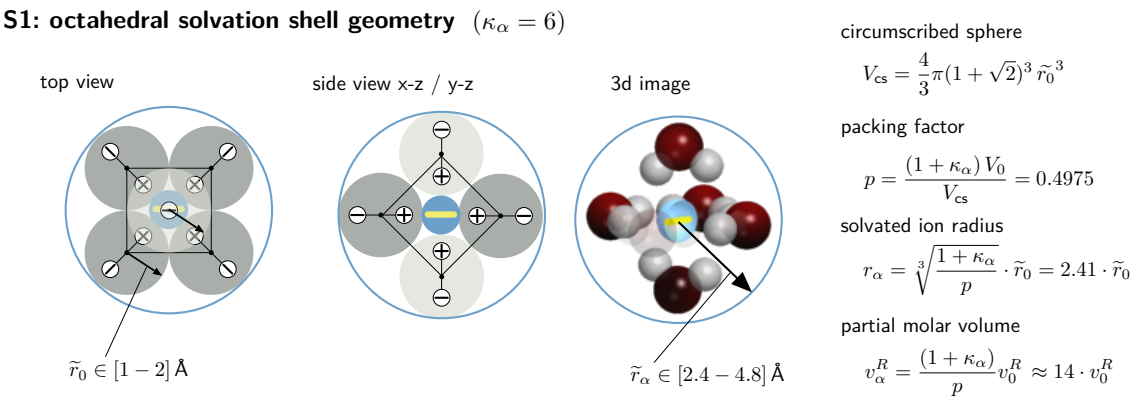

Figure 6: Octahedral molecular geometry with an anion in the centre and $\kappa_\alpha = 6$ solvent molecules on the coordination sites. The partial molar volume of the solvated ion computes as $v_\alpha^R \approx 14.07\, v_0^R$ and is thus much large than predicted by equation (53).

$\tilde{r}_0 \approx r_0$), we obtain

$$v_\alpha^R = \frac{1+\kappa_\alpha}{p}\, v_0^R = 14.07 \cdot v_0^R. \tag{56}$$

A comparison to the introductory relation (53) clearly shows the *origin* of the overestimating solvation number. For a given value of v_α^R we would obtain from (53) a solvation number of $\kappa_\alpha^{\text{eq.(53)}} = 13$, while the octahedral structure model (56) has a value of $\kappa_\alpha = 6$.

The packing factor can, of course, also be dependent on the actual ionic species $\mathrm{A}_\alpha^\pm$, and many structure models are imaginable with various solvation numbers are imaginable. Common is, however, that a reinterpretation of the solvation number based on the equation (53) might be misleading and that the central parameter for the capacity maximum is the partial molar volume.

Capacity measurements of the $\mathrm{KPF_6}$ and $\mathrm{KBF_4}$ [5, 27, 28] (c.f. Fig 7) show that the capacity maxima of the anodic and the cathodic branch are equal. Since neither of the constituents $\mathrm{K^+}$, $\mathrm{PF_6^-}$, $\mathrm{BF_4^-}$ adsorbs on silver, the capacity maxima of each branch is exclusively determined from the respective partial molar volume. The measured maxima are almost equal, which suggests $v_{\mathrm{K^+}}^R \approx v_{\mathrm{PF_6^-}}^R \approx v_{\mathrm{BF_4^-}}^R$. This finding also holds for many other small ionic species, like $\mathrm{H^+}, \mathrm{OH^-}, \mathrm{Na^+}, \mathrm{Cl^-}, \mathrm{ClO_4^-}, \mathrm{I^-}$.

From a first perspective this seems rather surprisingly. But the following discussion on the second solvation shell shows that it is indeed very like that the partial molar volumes are almost equal of many small ions.

Consider the structure model **S2** given in Fig. 8. The first solvation shell with $\kappa_\alpha^1 = 6$ solvent molecules is similar to the structure model **S1**. Around the first shell, a second one forms with 8 solvent molecules in the horizontal plane (top view). Above is another

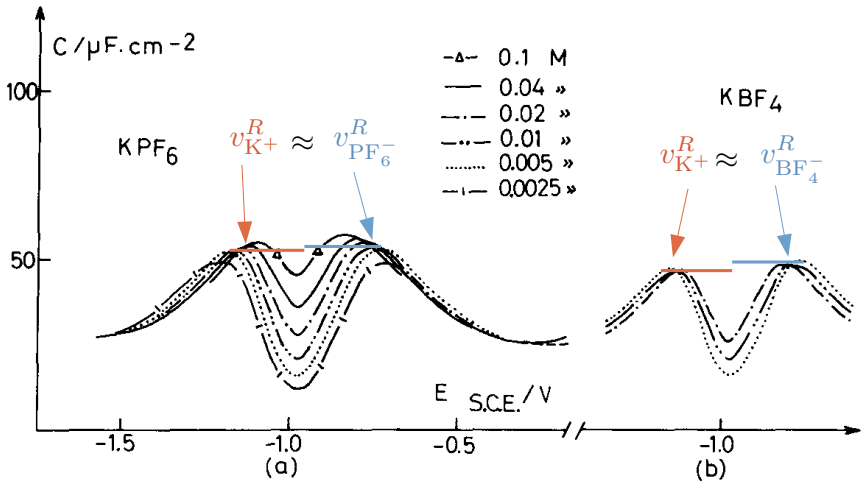

Figure 7: Capacity Fig 3. of [5] (Reprinted with permission of Elsevier).

ring of 4 solvent molecules is with an additional one on top. In both side views, this gives again a ring of 8 solvent molecules. This is a dense packed, highly symmetric structure model with $\kappa^2_\alpha = 18$ solvent molecules in the second solvation shell. In total, the solvation number is $\kappa^1_\alpha + \kappa^2_\alpha = 24$. The radius of the circumscribed sphere is $r_\alpha = \widetilde{r}_\alpha + 4 \cdot \widetilde{r}_0$, where $\widetilde{r}_\alpha$ is (again) the radius of the central ion itself, and $\widetilde{r}_0$ the radius of a solvent *sphere*. We obtain hence a packing factor $p = (1+\kappa^1_\alpha+\kappa^2_\alpha)/(\frac{\widetilde{r}_\alpha}{\widetilde{r}_0}+4)^3$ which is below 0.39.

Assuming now for the central ion a radius of $\widetilde{r}_\alpha = 1\,\text{Å}$, and for $\widetilde{r}_0$ again the molar radius $r_0 = 1.92\,\text{Å}$ leads to $v^R_\alpha = 91 \cdot v^R_0$, which seems to be a rather large value. However, as already mentioned above, the solvent radius $\widetilde{r}_0$ in the solvation shell is presumably smaller than the molar radius r_0 [29]. Using the radius of the water molecule itself, which is about $\widetilde{r}_0 = 1.5\,\text{Å}$, leads to $v^R_\alpha = 48 \cdot v^R_0$. This value is in remarkable agreement to our findings based on capacity maxima. A reinterpretation of $v^R_\alpha = 48 \cdot v^R_0$ in terms of eq. (53) would suggest 47 solvent molecules in the solvation shell since eq. (53) neglects the packing factor $p < 0.39$. But the structure model **S2** proposes $\kappa_\alpha = 24$, with $\kappa^1_\alpha = 6$ in the first shell and $\kappa^2_\alpha = 18$ in the second shell, which gives due to the packing factor a reasonable relation of $v^R_\alpha = 48 \cdot v^R_0$.

Of course, many more structure models are considerable, which lead to various solvation numbers and packing densities. Common to all is, however, the formation of two solvation shells which determine mainly the radius r_α of the solvated ion $\text{A}^\pm_\alpha$ and thus the partial molar volume $v^R_\alpha = \frac{4}{3}\pi r^3_\alpha$. Due to packing and symmetry reasons, the radius is at least $4 \cdot \widetilde{r}_0$, which already gives $v_\alpha = 30 \cdot v^R_0$ for $\widetilde{r}_0 = 1.5\text{Å}$ and $v_\alpha = 63 \cdot v^R_0$ for $\widetilde{r}_0 = 1.92\text{Å}$. The inner solvation shell captures $\kappa^1_\alpha = 4 - 8$ solvent molecules and the outer $\kappa^2_\alpha = 14 - 20$, which leads to packing fractions of $p = [0.28 - 0.44]$. Since the solvent radius in the solvation shell, $\widetilde{r}_0$, and molar radius, r_0, are presumably different (i.e. $\widetilde{r}_0 < r_0$), we have

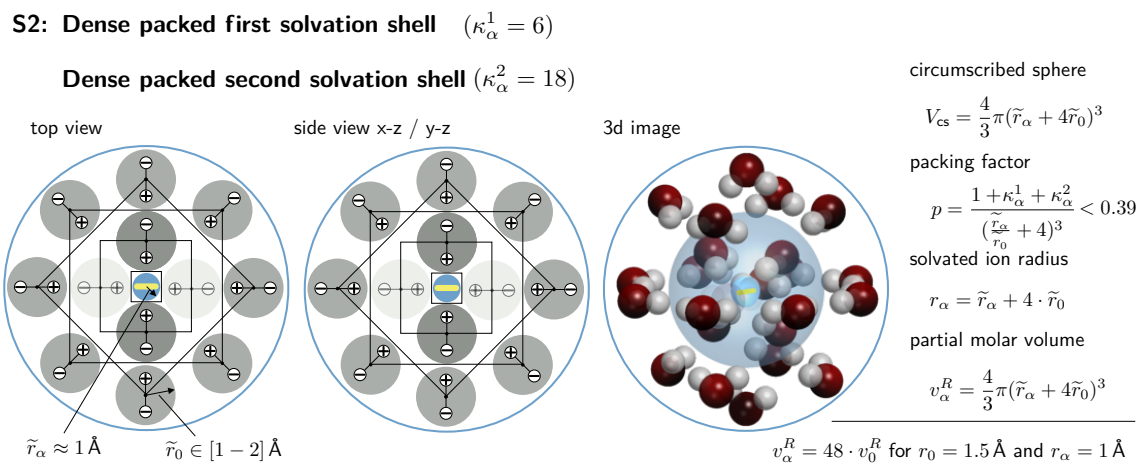

Figure 8: Structure model **S2** of a solvated anion with first and second solvation shell.

the general relation

$$v_\alpha^R = \frac{(1+\kappa_\alpha^1+\kappa_\alpha^2)}{p_\alpha}\left(\frac{\widetilde{r}_0}{r_0}\right)^3 \cdot v_0^R = \frac{1+\kappa_\alpha}{p_\alpha^{\text{eff}}} \cdot v_0^R = \omega_\alpha \cdot v_0^R \ . \tag{57}$$

The *effective* packing fraction p_α^{eff} covers the packing factor of the structure model as well as the influence of the reduced solvent radius in the solvation shell. The central remaining parameter is actually ω_α, which we call **ionic volume scaling factor** with respect to the solvent. For the representative structure model **S2** we have $p_\alpha^{\text{Eff}} \approx 0.52$ and $\kappa_\alpha = 24$, which leads to $\omega_\alpha = 48$. We can also compute the partial molar radius r_α of an ion based on the relation

$$r_\alpha = \sqrt[3]{\frac{3}{4\pi}v_\alpha^R} \approx 7\,\text{Å} \ , \tag{58}$$

which is in agreement to the findings of others, e.g. Freise [2]. We emphasize, however, that the interpretation of a *molar radius* r_α and its connection to a the solvation number κ_α is *difficile*.

3.1 Relationship to the ionic charge number

Since the microscopic origin of the solvation effect is actually the charge $e_0 z_\alpha$ of the central ion $\text{A}_\alpha^\pm$, it is expectably that the solvation number κ_α and the partial molar volume v_α^R depend on the charge number z_α [30, 31]. The microscopic origin of this relation is of course rather complex and not scope of this work. We rather seek a quantitative relationship between v_α^R and z_α in the light of the general relation (57), i.e. $v_\alpha^R = \omega_\alpha \cdot v_0^R$.

Consider completely dissociated solutions of AC , A_2C , and A_3C with equivalent concentration 0.01M. It is illustrative to consider three simple, representative models of the ionic volume scaling factor ω_α, i.e.

$$\text{M}_1 : \ \omega_\alpha = \omega_0 \ , \qquad \text{M}_2 : \omega_\alpha = |z_\alpha| \cdot \omega_0 \quad \text{and} \quad \text{M}_3 : \omega_\alpha = (z_\alpha)^2 \cdot \omega_0 \ , \tag{59}$$

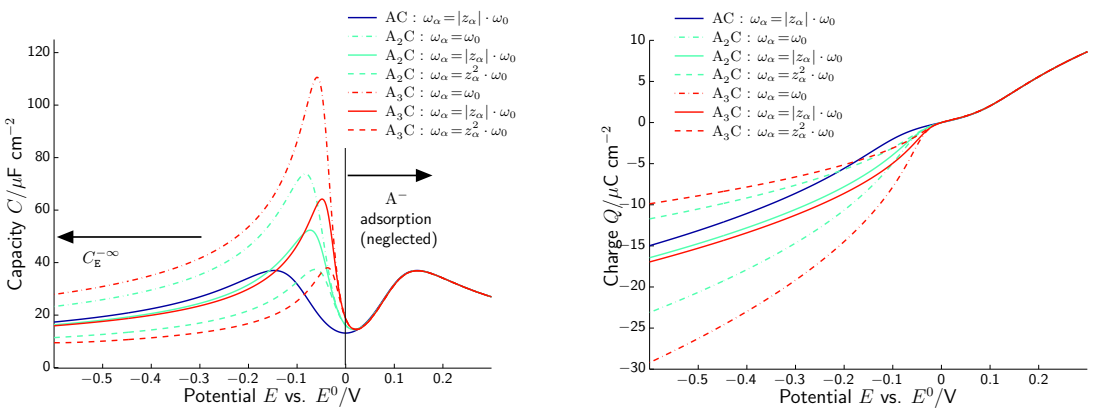

(a) Capacity

(b) Charge

Figure 9: Computed double layer capacity and charge of 0.01M AC , 0.005M $\mathrm{AC_2}$, 0.0033M $\mathrm{AC_3}$ aqueous solutions based on the thermodynamic model of section 2 and the solvation shell models (59) with $\omega_0 = 45$.

where ω_0 is a solvent specific quantity, and discuss their impact on the boundary layer capacity. Fig. 9a displays a computation of the capacity for the respective examples. It shows the complex interplay between charge number z_α of the anion and the partial molar volume of the respective models (59). Fig. 9b shows the corresponding double layer charge.

For $\mathrm{M}_1(\omega_\alpha = \omega_0)$ we find that the capacity maxima increase extremely (compared to the AC example) and that much more charge can be stored in the double layer (c.f. Fig. 9b). Since the partial molar volume of A^- , A^{2-} , and A^{3-} remains equal for this example, this is expectably as much more charge can be stored at a given amount of volume.

The model $\mathrm{M}_2(\omega_\alpha = |z_\alpha| \cdot \omega_0)$ shows a more intuitive behavior. The capacity maxima increases due to the increased charge number of the $\mathrm{AC_2}$ and $\mathrm{AC_3}$ anion. However, the capacity saturation $C_{\mathrm{E}}^{-\infty}$ at $E \to +\infty$ remains in the order of the AC value since the actual amount of charge stored in the double layer remains similar. This can be seen more clearly when one computes the charge density $q_{\mathrm{E}}(x)$, where x is the 1-D space variable normal to the metal surface, based on the equilibrium equation system (31),(32) and(36). Note that the canonical unit of $q_{\mathrm{E}}(x)$ is actually $\mu\mathrm{C\,cm^{-2}nm^{-1}}$ and remember that for a non-adsorbing salt $Q = -\int_0^{x_{\mathrm{E}}} q_{\mathrm{E}}\, dx$.

Figure 10 displays the numerical solutions of $q_{\mathrm{E}}(x)$, i.e. the space charge layer in the electrolyte, for the examples given above. The example AC can again be considered as reference since it was validated in [4] against experimental data of mono-valent salts.

For the model M_2 we find that the charge density in the Stern layer, i.e. the locally saturated anionic solution [1], remains almost equal for AC , $\mathrm{AC_2}$ and $\mathrm{AC_3}$. This

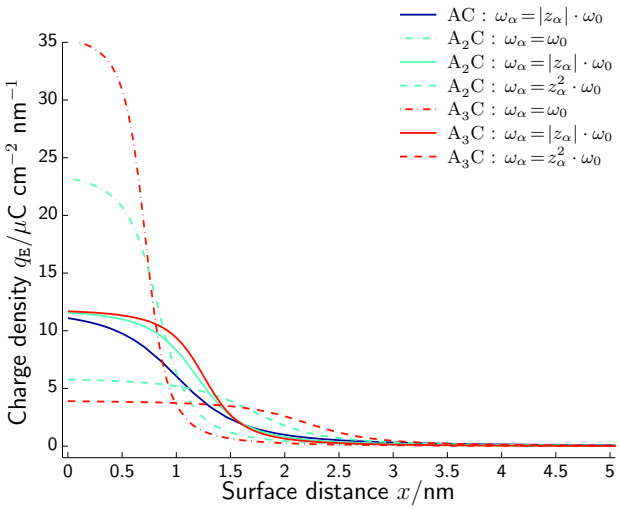

Figure 10: Space charge layer of 0.01M AC , 0.005M $\mathrm{AC_2}$, 0.0033M $\mathrm{AC_3}$ aqueous solutions based on the thermodynamic model of section 2 and the solvation shell models (59) with $\kappa_0 = 45$.

can also be understood by the representation of q_E, i.e.

$$q_\mathrm{E} = e_0 \frac{\sum_{\alpha=0}^{N_\mathrm{E}} z_\alpha \cdot y_\alpha}{\sum_{\alpha=0}^{N_\mathrm{E}} v_\alpha^R \cdot y_\alpha} \ . \tag{60}$$

If we have (local) saturation of the anion $\mathrm{A}^{(-,2-,3-)}$, i.e. $y_\mathrm{A} \to 1$ for $E \to \infty$ and thus $y_\alpha \to 0$ for all other species, we obtain $q_\mathrm{E}^\infty \to e_0 \frac{z_\mathrm{A}}{v_\mathrm{A}^R}$. Hence, for the model $\mathrm{M_2}$ this is essentially a constant, namely $q_\mathrm{E}^\infty \to e_0 \,\mathrm{sgn}(z_\mathrm{A}) \frac{1}{\omega_0 \, v_0^R}$. This explains why the saturation capacity $C_\mathrm{E}^{-\infty}$ almost coincide for AC , $\mathrm{AC_2}$ and $\mathrm{AC_3}$ for $\mathrm{M_2}$. The slight deviation arises from the slightly different Stern layer widths, c.f. Fig 10.

The model $\mathrm{M_3}(\omega_\alpha = (z_\alpha)^2 \cdot \omega_0)$ leads to almost equal capacity maxima for AC , $\mathrm{AC_2}$ and $\mathrm{AC_3}$, while the saturation capacity $C_\mathrm{E}^{-\infty}$ decreases (see Fig. 9a). This is in accordance with Fig. 9b, which shows that less charge is stored in the double layer compared to the AC example. Fig. 10 shows that for $\mathrm{M_3}$ the Stern layer widnes, however, storing less charge than the AC example.

Overall we conclude that a constant ionic volume scaling factor ω_α with respect to the charge number z_α underestimates the saturation capacity $C_\mathrm{E}^{-\infty}$, while a quadratic relation overestimates the value. For the relation $\omega_\alpha = \big|\,|z_\alpha|\,\big| \cdot \omega_0$ we obtain equal values for the saturation capacity $C_\mathrm{E}^{-\infty}$ for 0.01M AC , 0.005M $\mathrm{AC_2}$ and 0.00333M $\mathrm{AC_3}$. Quite surprisingly, D. Grahame observed this behavior alread in 1951 on a series of metallic chlorides dissolved in water [32]The capacity measurements were performed on mercury electrodes based on the experimental method explained in [33]. It is to emphasize that the adsorption of $\mathrm{Cl^-}$ can *hide* the capacity minimum of Fig. 9a, as well as differences in measurements to single crystal observations nowadays exist [34]. We focus here on the fact that the limiting values of the capacity, i.e. $C_\mathrm{E}^{-\infty}$, is almost equal for the aqueous

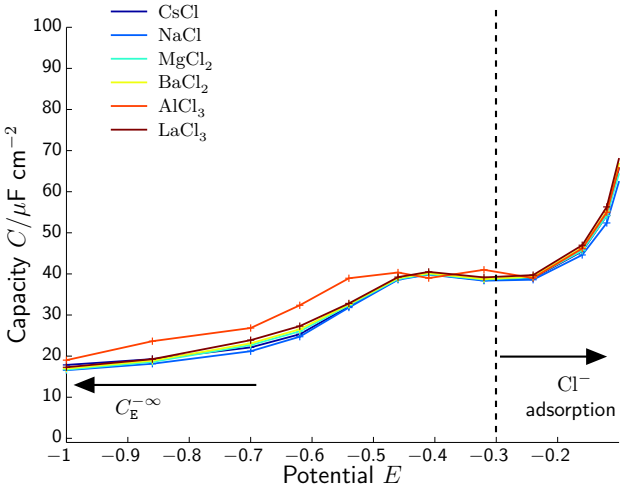

Figure 11: Experimentally measured capacity curves for 0.01M equivalent concentrations.

solutions of 0.01M NaCl , CsCl , 0.005M $\mathrm{MgCl_2}$, $\mathrm{BaCl_2}$, and 0.033M $\mathrm{AlCl_3}$. $\mathrm{LaCl_3}$. This is in accordance Fig. 9a with $\omega_\alpha = |z_\alpha| \cdot \omega_0$. Thus justifies our proposed relationship

$$v_\alpha^R = |z_\alpha| \cdot \omega_0 \cdot v_0^R \ , \tag{61}$$

where ω_0 is a solvent specific quantity. According to $(57)_2$, i.e.

$$\frac{1+\kappa_\alpha}{p_\alpha^{\text{eff}}} = |z_\alpha| \cdot \omega_0 \ , \tag{62}$$

the solvation number κ_α is thus also dependent on z_α. However, in order to actually determine the value of κ_α one would require a structure model for the multi-valent ions. If the effective packing density p_α^{eff} remains almost equal, i.e. $p_\alpha^{\text{eff}} \approx 0.5$, we observe that the solvation number κ_α increases linearly with the charge number z_α, i.e. from 24 for $z_\alpha = \pm 1$ to 48 for $z_\alpha = \pm 48$. This additional 24 solvent probably form a 3^{rd} solvation layer around the central ion. Note, however, that the packing density does not necessarily remain constant upon increasing the number of solvation shells.

Summarizing, we suggest thus for multi valent ion constitunes A_α with charge number z_α the relationship

$$v_\alpha^R = |z_\alpha| \cdot \omega_0 \cdot v_0^R \quad \text{with} \quad \omega_0 = 48 \tag{63}$$

and

$$\kappa_\alpha = \frac{1}{2} |z_\alpha| \, \omega_0 \ . \tag{64}$$

4 Partial molar area

On the metal surface we consider adsorbates $\underset{s}{\mathrm{A}}_{\alpha,\beta}$ in terms of surface species densities $\underset{s}{n}_{\alpha,\beta}$, originating from the adsorption, de-solvation and partial charge transfer reactions

(6)–(8), i.e. the net reactions

$$\mathrm{A}_\alpha + \sum_{\gamma=0}^{\beta} \mathrm{sgn}(z_\alpha)\lambda_{\alpha,\gamma}\cdot \mathrm{e}^- \rightleftharpoons \underset{s}{\mathrm{A}}_{\alpha,\beta} + (\kappa_\alpha - \underset{s}{\kappa}_{\alpha,\beta})\mathrm{A}_0 \qquad \beta = 0,1,\ldots,|z_\alpha|\,. \tag{65}$$

For each adsorbate we have in the thermodynamic equilibrium essentially two thermodynamic parameters which determine the amount of constituents on the surface, i.e.

- its partial molar area $a^R_{\alpha,\beta}$
- and the adsorption energy $\Delta\widetilde{g}^A_{\alpha,\beta}$.

In addition, the partial molar area of the metal surface a^R_M and the number of adsorption sites $\overline{\omega}_M$ each surface atom provides arise as model parameters. This encodes the different surface orientations, e.g. (111), (110), (100) or the liquid state.

For solid metal surfaces a^R_M is straight forward computed from the crystallographic structure of the considered surface orientation, e.g. for a fcc crystal with lattice distance ℓ_M we have

$$a^R_{M(111)} = \frac{\sqrt{3}}{8}(\ell_M)^2\,, \qquad a^R_{M(100)} = \frac{1}{2}(\ell_M)^2 \quad \text{and} \quad a^R_{M(110)} = \frac{\sqrt{2}}{2}(\ell_M)^2\,. \tag{66}$$

If each surface metal atom (or surface unit cell) provides one adsorption site (or vacancy) for all considered surface orientations (abc) we have $\overline{\omega}_M = 1$ whereby $a^R_{V(abc)} = a^R_{V(abc)}$ (**case a**). Note, however, that different surface orientations (abc) can potentially also offer different amounts $\omega_{M(abc)}$ of adsorption sites. It thus possible that a^R_V is equal for different surface orientations (abc), which implies that the metal partial molar area and the number of adsorption sites increase in a similar way, i.e. $a^R_V = \frac{1}{\overline{\omega}_{M(abc)}} a^R_{M(abc)}$ (**case b**). These two model perceptions become more clearly when the partial molar area of the adsorbates is discussed (see Fig. 12).

The specific molar area of the solvent is computed from

$$\widetilde{a}^R_0 = \frac{2}{\sqrt{3}}(2\,r_0)^2 \qquad \text{with} \quad r_0 = \sqrt[3]{\frac{3\pi}{4}v^R_0}, \tag{67}$$

which corresponds to a layer of densely packed spheres. For water this leads to a value of $\widetilde{a}^R_{\mathrm{H_2O}} = 10.33\cdot 10^8\ \frac{\mathsf{cm}^2}{\mathsf{mol}}$. The radius $r_0 = 1.92\,\text{Å}$ of the water molecule, or the packing density on the surface, can also be slightly different for the adsorbed state, which has accordingly an impact on $\widetilde{a}^R_{\mathrm{H_2O}}$. Parsons *et. al* [35] introduce a value of $\hat{a}^R_{\mathrm{H_2O}} = 7.40723\cdot 10^8\ \frac{\mathsf{cm}^2}{\mathsf{mol}}$ which originates from this circumstance. Both values are in the same range and we proceed our discussion with $\widetilde{a}^R_{\mathrm{H_2O}}$.

However, even more crucial is the question wether the thermodynamic parameter, i.e. the partial molar area a^R_0, is influenced by the lattice structure on which the constituent is adsorbed. Two extreme cases are imaginable:

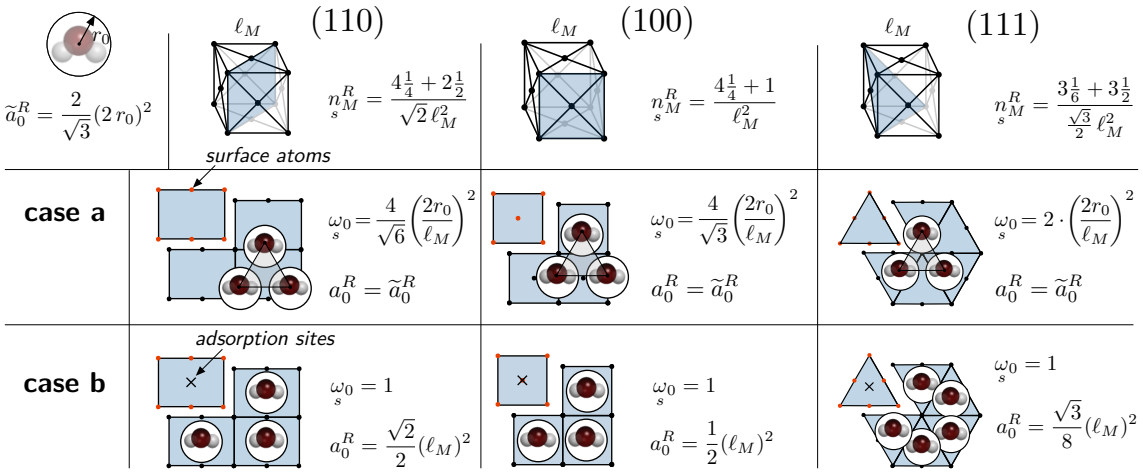

Figure 12: Different number of adsorption sites on different metal surfaces can lead to the same partial molar area a_0^R of an adsorbate.

- the partial molar area a_0^R remains equal for different surface orientations (**case a**),
- and each surface atom provides one adsorption site (**case b**).

Figure 12 sketches the different model perceptions. Whether **case a** or **b** is physically meaningful cannot be directly answer from continuum thermodynamics itself. Both cases are thermodynamically consistent. However, we expect the surface density $\underset{s}{\rho} \approx m_0 \underset{s}{n}_0$ of the solvent to remain equal for different surface structures. This is corresponds to **case a**, whereby the partial molar area $a_0^R = \tilde{a}_0^R$ is equal for different metal surfaces, orientations and states.

Next we discuss the partial molar area $a_{\alpha,\beta}^R$ of the ionic species on the surface. Expectably, the preceding discussion on the partial molar volume v_α^R and the impact of the solvation effect holds in a similar way for $a_{\alpha,\beta}^R$. i.e. two-dimensional surface solvation [36, 37]. Hence, in order to relate the solvation numbers $\underset{s}{\kappa}{}_{\alpha,\beta}^1$ and $\underset{s}{\kappa}{}_{\alpha,\beta}^2$ of the first and second (surface) solvation shell to the partial molar area, some structure model for adsorbed ions is required. It is not the scope of this work to actually predict different structure models. We rather discuss some aspects of representative structure models and their impact on the thermodynamic parameter $a_{\alpha,\beta}^R$.

Summarizing, this means that we have a relationship

$$a_{\alpha,\beta}^R = \frac{1+\underset{s}{\kappa}_{\alpha,\beta}}{\underset{s}{p}{}_{\alpha,\beta}^{\mathsf{Eff}}} \cdot a_0^R = \underset{s}{\omega}_{\alpha,\beta} \cdot a_0^R \ , \tag{68}$$

where $\underset{s}{\kappa}_{\alpha,\beta} = \underset{s}{\kappa}{}_{\alpha,\beta}^1 + \underset{s}{\kappa}{}_{\alpha,\beta}^2$ denotes the surface solvation number, $\underset{s}{p}{}_{\alpha,\beta}^{\mathsf{Eff}}$ the effective packing density, and $\underset{s}{\omega}_{\alpha,\beta}$ the ionic area scaling factor with respect to the solvent. The ionic area

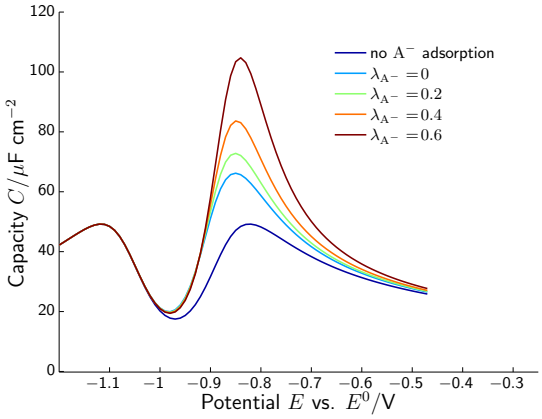

(a) Computation of the double layer capacity for a 0.1M aqueous solution of AC subject to a partial charge transfer reaction 70 on the surface.

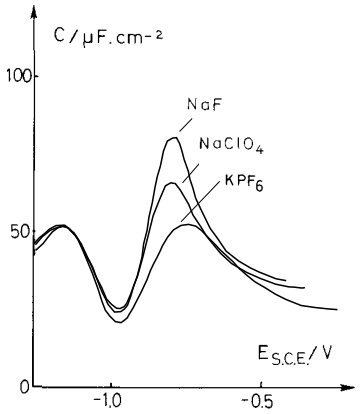

(b) Data of Valette [5], for 0.01M solutions of NaF , $\mathrm{KPF_6}$, and $\mathrm{NaClO_4}$ (reprinted with permission from Elsevier)

Figure 13: Comparison of computed and experimental capacity curves.

scaling factor is expectably also related to the charge number of the central ion, i.e.

$$\underset{s}{\omega}_{\alpha,\beta} = \left|\underset{s}{z}_{\alpha,\beta}\right| \cdot \underset{s}{\omega}_0 \ , \tag{69}$$

where ω_0 is again a solvent specific quantity. Note, however, that $\underset{s}{\omega}_{\alpha,\beta} = \left|\underset{s}{z}_{\alpha,\beta}\right| \cdot \underset{s}{\omega}_0$ would imply $a^R_{\alpha,\beta} \to 0$ for an uncharged adsorbate $\underset{s}{z}_{\alpha,\beta} \to 0$, which is certainly not correct. We would rather expect $a^R_{\alpha,\beta} \to \tilde{a}^R_\alpha$ for $\underset{s}{z}_{\alpha,\beta} \to 0$, where $\tilde{a}^R_\alpha$ is the partial molar area of the (uncharged) central ion itself. We expect thus that the relation (69) holds up to some lower limit, employed here as $\left|\underset{s}{z}_{\alpha,\beta}\right| > 0.2$.

Remember that the charge number of $\underset{s}{\mathrm{A}}_{\alpha,\beta}$ could be fractional, i.e. $\underset{s}{z}_{\alpha,\beta} = z_\alpha - \sum_{\gamma=0}^{\beta} \mathrm{sgn}(z_\alpha)\lambda_{\alpha,\gamma}$, due to the partial charge transfer reaction (65). The partial charge transfer coefficients $\lambda_{\alpha,\gamma}$ assume fractional values between -1 and 1. Consequently the partial molar area of an ionic adsorbate is related to $\lambda^\beta_\alpha = \sum_{\gamma=0}^{\beta} \lambda_{\alpha,\gamma}$.

We discuss the impact of partial charge transfer on the double layer capacity for some aqueous ionic solution AC. The mono-valent anion A^- is assumed to adsorb on the metal surface, which is accompanied by a partial charge transfer and some restructuring of the solvation shell, i.e.

$$\mathrm{A}^- - \lambda_{\mathrm{A}}\mathrm{e}^- \rightleftharpoons \underset{s}{\mathrm{A}}^- + (\kappa_{\mathrm{A}^-} - \underset{s}{\kappa}_{\mathrm{A}^{1-\lambda}})\mathrm{H_2O} \ . \tag{70}$$

The contribution of $\underset{s}{\mathrm{A}}^-$ for values of $\lambda_{\mathrm{A}^-} \in [0, 0.6]$ based on the model (69) on the capacity is displayed in Fig. 13a

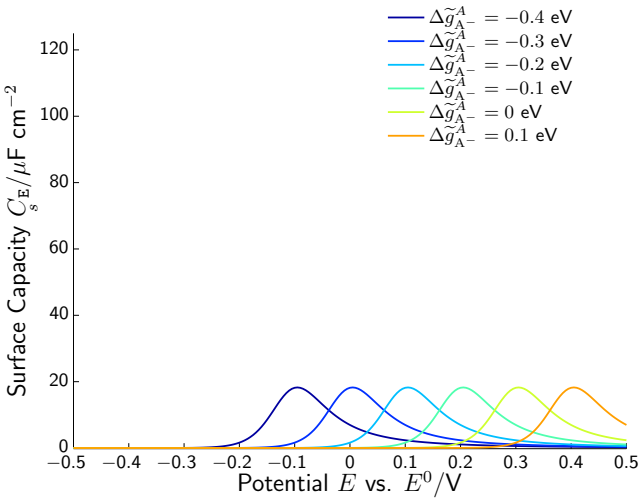

Figure 14: Computation of the surface capacity with $a^R_{\mathrm{A}^-} = 30 \cdot a^R_0$ and a parameter variation of Δg_{A^-}.

Consider KPF_6 as reference of a non-adsorbing salt and NaClO_4, NaF as examples with adsorbing anions. The measurement of Valette shows that the surface capacity contribution of ClO^{4-} smaller than F^-. From a thermodynamic point of view, the only parameter which determines the surface capacity maximum is actually the partial molar area a^R_α of the respective adsorbate. Since both ions have an equal solvation shell in the volume, c.f. the prior discussion, one would *a priori* assume that a similar behavior also holds at the surface. But this obviously not the case, and Fig. 3a is the experimental evidence that the molar area of F^- is smaller than ClO^{4-}.

What is the origin of this *shrinking*? Note that thermodynamically a statement like " F^- binds stronger on the metal surface than ClO_4^- " actually only has an impact on $\Delta\widetilde{g}^A_\alpha$, which shifts the (surface) capacity maximum to the left or right (see Fig. 14), but does not influence the value of the maximum. Thus, "a stronger binding" cannot be the origin.

If one assumes, however, that the partial molar area is related to the charge $\underset{s}{z}_{\mathrm{A}^-} = z_{\mathrm{A}^-} + \lambda_{\mathrm{A}^-}$ an adsorbate $\underset{s}{\mathrm{A}}^-$ actually carries, i.e. relation (69), the effect of a shrinking molar area is naturally explained by some partial charge transfer! Due the charge transference, the dipole interaction between the outer solvent molecules decreases and the ion strips of a part of the solvation shell whereby it *shrinks*. We can thus understand the difference between F^- and ClO^{4-} in terms of different amounts of partially transferred charge on the adsorbed ions.

However, in comparison to measured data of G. Valette [5] we find that the concept of partial charge transfer explains quite well the increasing (surface) capacity, and we finalize the discussion with a representative structure model.

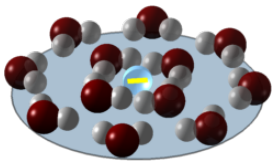

(a) Slice of the structure model **S2** as surface structure model.

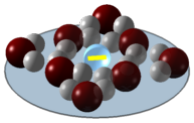

(b) Sketch of an adsorbed ion with smaller solvation shell.

Figure 15: Sketches of two different ionic surface structure models with different solvation numbers and molar radii.

Of course, our modeling procedure does not pretend to predict any structures of the adsorbed ions. We provide rather a thermodynamically consistent interpretation (or mechanism) why the partial molar areas of two adsorbed ions can be different. The interaction between the central ion and solvent molecules on a surface can be far more complex, since electrostatic interactions in 2D are inherently different from 3D. But any surface thermodynamic theory requires explicit values for the partial molar area of ionic adsorbates. The most simple approach is to assume that an ionic adsorbate for which no partial charge is transferred has a similar molar radius than the respective ion in solution, i.e. $r_\alpha \approx 7\,\text{Å}$. If we compute now the partial molar area based on the relation

$$a_\alpha^R = 4\pi r_\alpha^2 \approx 36 \cdot a_0^R \;, \tag{71}$$

we find actually an ionic scaling factor of $\underset{s}{\omega}_\alpha = 36$ (for mono-valent ions). This value is in surprisingly good agreement to surface capacity data of G. Valette [5] on $\mathrm{NaClO_4}$, in the sense that our model predicts capacity maxima which are almost equal to the measured data. However, in order to determine the actual solvation number based on the relation (68), one requires a packing density and thus a structure model. If we consider the solvated ion as one once slice to the structure model **S2** (top view), we obtain a solvation number of $\kappa = 8 + 4 = 12$ and thus an effective packing density of $\underset{s}{p}_\alpha^{\text{Eff}} \approx 0.36$ (c.f. Fig. 15a). Compared to the effective packing density $p_\alpha \approx 0.52$ this means that adsorbed ions haven an even lesser dense packed solvation shell.

However, we employ thus a value of $\underset{s}{\omega}_0 = 36$ for the solvent specific ionic scaling factor together with the model perception $\underset{s}{\omega}_\alpha = \left|\underset{s}{z}_\alpha\right| \cdot \underset{s}{\omega}_0$ for adsorbed, solvated, partially charged ions.

For a transferred charge of $\lambda_{\mathrm{A}^-} = 0.4$ we obtain hence a value of $\underset{s}{\omega}_{\mathrm{A}^-} = 0.6 \cdot 36 = 21.6$, or, retranslated in terms of a molar radius, a value of $r_\alpha \approx 5.42\text{A}$. If the effective packing density $\underset{s}{p}_{\mathrm{A}^-}^{\text{Eff}}$ remains almost equal for the partially charged ion (which is not necessarily the case), we obtain a solvation number of $\kappa_{\mathrm{A}^-} \approx 8$. This value is probably a little bit bigger since the packing density increases for smaller solvation shells. However, the resulting values are quite meaningful for adsorbed F^- , and the concept of partial charge transfer in combination with the molar area explains naturally the increasing surface capacity of NaF compared to $\mathrm{NaClO_4}$.

5 Summary

Based on the general framework of non-equilibrium thermodynamics for volumes and surfaces we derived representations of the boundary layer $C_{\mathrm{E}}^{\mathrm{BL}}$ and the surface capacity $\underset{s}{C}_{\mathrm{E}}$, which form together the measureable double layer capacity $C_{\mathrm{E}} = C_{\mathrm{E}}^{\mathrm{BL}} + \underset{s}{C}_{\mathrm{E}}$. It turns out that the crucial parameters for $C_{\mathrm{E}}^{\mathrm{BL}}$ is the partial molar volume v_α^R of the ionic constituents, while for $\underset{s}{C}_{\mathrm{E}}$ the partial molar area a_α^R is the dominant parameter. Both values determine the respective capacity maximum.

Due to the solvation effect, i.e. the binding of κ_α, $\underset{s}{\kappa}_\alpha$ solvent molecules to the central ion, the molar volume and area of an ionic constituent A_α increase, where the most simple relations are

$$v_\alpha^R = (1 + \kappa_\alpha) \cdot v_0^R \quad \text{and} \quad a_\alpha^R = (1 + \underset{s}{\kappa}_\alpha) \cdot a_0^R, \tag{72}$$

with v_0^R / a_0^R being the molar volume/area of the solvent. However, it turns out that these simple relations have quite some shortcomings and lead to a misinterpretation of the actual values for $\kappa_\alpha / \underset{s}{\kappa}_\alpha$. It is thus more illustrative to consider initially relations

$$v_\alpha^R = \omega_\alpha \cdot v_0^R \quad \text{and} \quad a_\alpha^R = \underset{s}{\omega}_\alpha \cdot a_0^R, \tag{73}$$

where $\omega_\alpha / \underset{s}{\omega}_\alpha$ are the *ionic scaling factors*. Measurement of the double layer capacity on single crystal silver electrodes suggest values of $\omega_\alpha \in [40 - 50]$ and $\underset{s}{\omega}_\alpha \in [10 - 40]$ [4]. Obviously, these values seem to overestimate the solvation numbers based on the relations (72). Requisitioning the relations (72) actually shows that these neglect packing effects. While the important thermodynamic parameters for the double layer capacities are actually ω_α and $\underset{s}{\omega}_\alpha$, which certainly incorporate the solvation numbers of the respective ion, the determination of actual values for κ_α and $\underset{s}{\kappa}_\alpha$ requires some structure models for mono-valent ions. For representative structure model we showed that a more realistic relation between the partial molar volume/area and the solvation numbers is

$$v_\alpha^R = \frac{(1 + \kappa_\alpha)}{p_\alpha^{\mathsf{Eff}}} \cdot v_0^R \quad \text{and} \quad a_\alpha^R = \frac{(1 + \underset{s}{\kappa}_\alpha)}{\underset{s}{p}_\alpha^{\mathsf{Eff}}} \cdot a_0^R, \tag{74}$$

where $p_\alpha^{\mathsf{Eff}} \, / \underset{s}{p}_\alpha^{\mathsf{Eff}}$ are the effective packing densities of the solvation shell. For spherical ions in the volume this value is about $p_\alpha^{\mathsf{Eff}} \approx 0.52$, while on the surface the solvation shell is lesser dense packed with $\underset{s}{p}_\alpha^{\mathsf{Eff}} \approx 0.36$. For both, volumetric and surface solvated ions, we can compute the partial molar radius, i.e.

$$r_\alpha = \sqrt[3]{\frac{3}{4\pi} v_\alpha^R} \approx \sqrt{\frac{1}{4\pi} a_\alpha^R} \, , \tag{75}$$

for which we obtain reasonable values of $r_\alpha \approx 7\text{Å}$.

When multi-valent ions are discussed, the question arises how the partial molar volume is related to charge number of the ion. Our discussion suggests relations

$$v_\alpha^R = |z_\alpha|\ \omega_0 \cdot v_0^R \quad \text{and} \quad a_\alpha^R = \left| \underset{s}{z}_\alpha \right|\ \underset{s}{\omega}_0 \cdot a_0^R\ , \tag{76}$$

where ω_0 and $\underset{s}{\omega}_0$ are solvent specific ionic scaling factors. Based on a comparison to experimental date we obtain for water as solvent $\omega_0 = 48$ and $\underset{s}{\omega}_0 = 36$ (which leads to $r_\alpha = 7\,\text{Å}$ for mono-valent ions). This linear relationship between the partial molar volume v_α^R and the charge number z_α predicts almost equivalent values for the capacity limit $C_{\text{E}}(E \to -\infty)$ for equivalent solutions of AC, A_2C and A_3C. This finding is underpinned by experimental data of Grahame on a series of metallic chlorides, namely $0.01\text{M}\ \ \text{NaCl}$, CsCl , $0.005\text{M}\ \ \text{MgCl}_2$, BaCl_2 , and $0.033\text{M}\ \ \text{AlCl}_3$. LaCl_3 , which show exactly this behavior: The double layer capacity is almost equal for all solutions (in range of experimental error).

Finally, when an ion A^- adsorbs on a metal surface, the question arises if this adsorption process is, or could be, accompanied with some partial charge transfer, i.e. $\text{A}^- + \lambda_\text{A} \cdot e^- \rightleftharpoons \text{A}^{1-\lambda}$. It turns out that neither the equilibrium representation of the surfactants nor the measurable effective surface charge density depend on the partial charge transfer coefficient λ_A. However, in the light of the relation (76) the surface capacity becomes *naturally* (mathematically: parametric) dependent on λ_A, since $\underset{s}{z}_\text{A} = z_\text{A} - \lambda_\text{A}\,\text{sgn}(z_\text{A})$. The relation (76) actually states that the partial molar area decreases when the charge of the central ion decreases. Origin of this is the shrinking solvation shell is thus the partial charge transfer. This mechanism explains very well the difference in capacity values of NaClO_4 and NaF , and attributes this difference to the partial charge transfer and the shrinking partial molar area.

References

[1] W. Dreyer, C. Guhlke and M. Landstorfer, *Electrochemistry Communications*, 2014, **43**, 75 – 78.

[2] V. Freise, *Zeitschrift für Elektrochemie, Berichte der Bunsengesellschaft für physikalische Chemie*, 1952, **56**, 822–827.

[3] J. Bikerman, *Philosophical Magazine Series 7*, 1942, **33**, 384–397.

[4] M. Landstorfer, C. Guhlke and W. Dreyer, *Electrochimica Acta*, 2016, **201**, 187 – 219.

[5] G. Valette, *Journal of Electroanalytical Chemistry and Interfacial Electrochemistry*, 1981, **122**, 285 – 297.

[6] J. Meixner and H. G. Reik, in *Thermodynamik der irreversiblen Prozesse*, Springer, Berlin, 1959, vol. 3, pp. 413–523.

[7] I. Müller, *Thermodynamics*, Pitman Advanced Publishing Program, Boston, 1985.

[8] S. de Groot and P. Mazur, *Non-Equilibrium Thermodynamics*, Dover Publications, 1984.

[9] D. Bothe and W. Dreyer, *Acta Mechanica*, 2014, 1–49.

[10] D. Bedeaux, in *Advances in Chemical Physics*, ed. P. Ilya and S. A. Rice, John Wiley Sons, Inc., 1986, vol. 64, pp. 47–109.

[11] C. Guhlke, *Ph.D. thesis*, TU Berlin, 2015.

[12] M. Landstorfer, *Ph.D. thesis*, Universität Ulm, 2013.

[13] W. Schmickler and R. Guidelli, *Electrochimica Acta*, 2014, **127**, 489 – 505.

[14] W. Lorenz and G. Salié, *Journal of Electroanalytical Chemistry and Interfacial Electrochemistry*, 1977, **80**, 1 – 56.

[15] J. Bockris, A. Reddy and M. Gamboa-Aldeco, *Modern Electrochemistry 2A: Fundamentals of Electrodics*, Kluwer Academic Publishers, 2002.

[16] Y. Marcus, *J. Chem. Soc., Faraday Trans.*, 1991, **87**, 2995–2999.

[17] H. G. Hertz, *Angewandte Chemie International Edition in English*, 1970, **9**, 124–138.

[18] J. F. Hinton and E. S. Amis, *Chemical Reviews*, 1971, **71**, 627–674.

[19] R. Dogonadze and A. Kornyshev, *Journal of the Chemical Society*, 1974.

[20] S. Zhao, R. Ramirez, R. Vuilleumier and D. Borgis, 2011, **134**, 194102.

[21] D. M. Kolb, *Angewandte Chemie*, 2001, **113**, 1198–1220.

[22] C. Hamann and W. Vielstich, *Elektrochemie*, John Wiley & Sons Australia, Limited, 2005.

[23] S. Woelki and H.-H. Kohler, *Chemical Physics*, 2000, **261**, 421 – 438.

[24] K. J. Tielrooij, N. Garcia-Araez, M. Bonn and H. J. Bakker, *Science*, 2010, **328**, 1006–1009.

[25] Z. Bo, H. Yang, S. Zhang, J. Yang, J. Yan and K. Cen, *Scientific reports*, 2015, **5**, year.

[26] R. I. Slavchov and T. I. Ivanov, *The Journal of Chemical Physics*, 2014, **140**, year.

[27] G. Valette, *Journal of Electroanalytical Chemistry and Interfacial Electrochemistry*, 1989, **269**, 191 – 203.

[28] G. Valette, *Journal of Electroanalytical Chemistry and Interfacial Electrochemistry*, 1982, **138**, 37 – 54.

[29] I. Waluyo, C. Huang, D. Nordlund, U. Bergmann, T. M. Weiss, L. G. M. Pettersson and A. Nilsson, *The Journal of Chemical Physics*, 2011, **134**, year.

[30] L. G. Hepler, *The Journal of Physical Chemistry*, 1957, **61**, 1426–1429.

[31] L. G. Hepler, J. M. Stokes and R. H. Stokes, *Trans. Faraday Soc.*, 1965, **61**, 20–29.

[32] D. C. Grahame, *Journal of The Electrochemical Society*, 1951, **98**, 343–350.

[33] D. C. Grahame, *Journal of the American Chemical Society*, 1941, **63**, 1207–1215.

[34] J. Bockris, B. Conway and E. Yeager, *Comprehensive treatise of electrochemistry*, Springer, 1980, vol. 1: The Double Layer.

[35] J. Lawrence and R. Parsons, *The Journal of Physical Chemistry*, 1969, **73**, 3577–3581.

[36] B. Conway, *Electrochimica Acta*, 1995, **40**, 1501 – 1512.

[37] S. Meng, D. V. Chakarov, B. Kasemo and S. Gao, *The Journal of chemical physics*, 2004, **121**, 12572–12576.

A Explicit capacity representations

A.1 Boundary layer capacity

Reconsider the definition of $q_{\mathrm{E}}^{\mathrm{BL}}$, i.e.

$$q_{\mathrm{E}}^{\mathrm{BL}} = \int_{s}^{x_{\mathrm{E}}^{\mathrm{DL}}} q_{\mathrm{E}}\, dx \ . \tag{77}$$

Within the boundary layer we have the representation [4]

$$\partial_x \varphi = -\operatorname{sgn}(\varphi - \varphi^{\mathrm{E}}) \sqrt{\frac{2}{\varepsilon_0(1+\chi_{\mathrm{E}})}\big(p - p_{\mathrm{E}}\big)} \tag{78}$$

one obtains

$$q_{\mathrm{E}}^{\mathrm{BL}} = -\operatorname{sgn}(U_{\mathrm{E}}) \sqrt{2\varepsilon_0(1+\chi_{\mathrm{E}})\big(p\big|_{s}^{x} - p_{\mathrm{E}}\big)}, \tag{79}$$

where $p\Big|_{\substack{x\\s}} = \hat{p}(U_{\mathrm{E}})$ is obtained from the implicit equation system

$$g(U,p) = \sum_{\alpha\in\mathcal{I}_{\mathrm{E}}} y_\alpha(\varphi,p) - 1 = 0 \ . \tag{80}$$

with representations 36 of y_α. The functional representation of the pressure p satisfies

$$\frac{d\hat{p}}{d\varphi} = -q_{\mathrm{E}} \ , \tag{81}$$

leading to

$$C_{\mathrm{E}}^{\mathrm{BL}} = -\,\mathrm{sgn}(\varphi-\varphi^{\mathrm{E}})\sqrt{\frac{\varepsilon_0(1+\chi_{\mathrm{E}})}{2\big(\hat{(}U_{\mathrm{E}})-p^{\mathrm{E}}\big)}\cdot q_{\mathrm{E}}(U_{\mathrm{E}},\hat{p}(U_{\mathrm{E}}))\big(p-p^{\mathrm{E}}\big)} \ . \tag{82}$$

A.2 Surface capacity

Here we provide a semi-explicit representation of the surface capacity $\underset{s}{C}$. First of all note that the surface charge $\underset{s}{q}$ has the representation

$$\underset{s}{q} = -\frac{\sum_{\alpha=1}^{N_{\mathrm{E}}} z_\alpha e_0 \underset{s}{y_\alpha} + \sum_{\alpha=1}^{N_{\mathrm{E}}}\sum_{\beta=-1}^{|z_\alpha|} z_\alpha e_0 \underset{s}{y_{\alpha,\beta}}}{a_V^R \underset{s}{y_V} + \sum_{\alpha=0}^{N_{\mathrm{E}}} a_\alpha^R \underset{s}{y_\alpha} + \sum_{\alpha=0}^{N_{\mathrm{E}}}\sum_{\beta=-1}^{|z_\alpha|} a_{\alpha,\beta}^R \underset{s}{y_{\alpha,\beta}}} \ . \tag{83}$$

With the representations (42) for $\underset{s}{y_\alpha}$, $\underset{s}{y_{\alpha,\beta}}$ and $\underset{s}{y_V}$ we obtain an expression of $\underset{s}{q}$ in terms of $(\underset{s}{\varphi}-\varphi^{\mathrm{E}})$ and $(\gamma-\gamma^R)$, i.e. $\underset{s}{q} = \underset{s}{\hat{q}}(\underset{s}{\varphi}-\varphi^{\mathrm{E}},\gamma-\gamma^R)$. The surface charge is thus a function of $\underset{s}{\varphi}$ **and** the surface tension γ. The surface fractions $\underset{s}{y_{\alpha,\beta}}$ obey the constraint

$$\underset{s}{y_V}(\gamma-\gamma^R) + \sum_{\alpha=0}^{N_{\mathrm{E}}} \underset{s}{y_\alpha}(\underset{s}{\varphi}-\varphi^{\mathrm{E}},\gamma-\gamma^R) + \sum_{\alpha=0}^{N_{\mathrm{E}}}\sum_{\beta=-1}^{|z_\alpha|} \underset{s}{y_{\alpha,\beta}}(\underset{s}{\varphi}-\varphi^{\mathrm{E}},\gamma-\gamma^R) - 1 = 0 \ , \tag{84}$$

which is an implicit relationship between U_{E} and $\gamma-\gamma^{\mathrm{R}}$. Hence, we may use the implicit function theorem to deduce a solution $\gamma = \hat{\gamma}(U_{\mathrm{E}})$ from equation (84), which satisfies $d\hat{\gamma}/d(U_{\mathrm{E}}) = \underset{s}{q}$. The surface capacity $\underset{s}{C}$ is thus

$$\underset{s}{\hat{C}} = \frac{d\underset{s}{\hat{q}}}{dU_{\mathrm{E}}} = \Big(\frac{\partial \underset{s}{q}}{\partial U_{\mathrm{E}}} + \underset{s}{q}\cdot\frac{\partial \underset{s}{q}}{\partial(\gamma-\gamma^R)}\Big). \tag{85}$$

With the (dimensionless) abbreviations

$$\underset{s}{f_1} := \sum_{\alpha=1}^{N_E} z_\alpha \underset{s}{y_\alpha} + e_0 \sum_{\alpha=1}^{N_E} \sum_{\beta=-1}^{|z_\alpha|} z_\alpha \underset{s}{y_{\alpha,\beta}} \tag{86}$$

$$\underset{s}{f_2} := \underset{s}{y_V} + \omega_0 \underset{s}{y_0} + \sum_{\alpha=1}^{N_E} \omega_\alpha \underset{s}{y_\alpha} + \sum_{\alpha=1}^{N_E} \sum_{\beta=-1}^{|z_\alpha|} \omega_{\alpha,\beta} \underset{s}{y_{\alpha,\beta}} \tag{87}$$

$$\underset{s}{f_3} = \sum_{\alpha=1}^{N_E} z_\alpha^2 \underset{s}{y_\alpha} + \sum_{\alpha=1}^{N_E} \sum_{\beta=-1}^{|z_\alpha|} z_\alpha^2 \underset{s}{y_{\alpha,\beta}} \tag{88}$$

$$\underset{s}{f_4} = e_0 \sum_{\alpha=1}^{N_E} z_\alpha \ \omega_\alpha \ \underset{s}{y_\alpha} + e_0 \sum_{\alpha=1}^{N_E} \sum_{\beta=-1}^{|z_\alpha|} z_\alpha \ \omega_{\alpha,\beta} \ \underset{s}{y_{\alpha,\beta}} \tag{89}$$

$$\underset{s}{f_5} = \underset{s}{y_V} + \omega_0 \underset{s}{y_0} + \sum_{\alpha=1}^{N_E} \omega_\alpha \underset{s}{y_\alpha} + \sum_{\alpha=1}^{N_E} \sum_{\beta=-1}^{|z_\alpha|} \omega_{\alpha,\beta}^2 \underset{s}{y_{\alpha,\beta}} \tag{90}$$

we obtain for the surface capacity the expression

$$\underset{s}{\hat{C}} = -\frac{e_0^2}{k_B T a_V^R} \left(\frac{\underset{s}{f_1} \cdot \underset{s}{f_4} - \underset{s}{f_3} \cdot \underset{s}{f_2}}{(\underset{s}{f_2})^2} + \frac{\underset{s}{f_1}}{\underset{s}{f_2}} \frac{\underset{s}{f_4} \cdot \underset{s}{f_2} - \underset{s}{f_1} \cdot \underset{s}{f_5}}{(\underset{s}{f_2})^2} \right). \tag{91}$$

Note that the term $\frac{e_0^2}{k_B T a_V^R}$ indeed has units $\frac{\mathsf{F}}{\mathsf{m}^2}$ and that all functions $\underset{s}{f_k}, k = 1, \ldots, 5$, are dependent on U_E **and** $\gamma - \gamma^R$.